PEOPL's DEMOCRATIC REPUBLIC OF ALGERIA
MINISTRY OF HIGHER EDUCATION AND SCIENTIFIC RESEARCH

Mohamed Boudiaf university of Msila
Faculty of Mathematics and computer sciences
Department of Mathematics

Master's thesis

Field : Mathematics and computer sciences
Branch : Mathematics
Option : Partial Differential Equations and its Applications

Theme

Approximate Solutions for Time-Fractal Fractional Differential Equations

Presented by :
Miss LAMRI Ouarda

Publicly supported on :June 04, 2026.

In front of the jury composed of :

FERAHTIA Nassim	MCB,	Mohamed Boudiaf University of M′sila	**President**.
ABDELKEBIR Saad	MCA,	Mohamed Boudiaf University of M′sila	**Supervisor.**
BENMEDDOUR Mohamed Ourabah	MCB,	Mohamed Boudiaf University of M′sila	**Examiner.**

University year 2025/2026

Acknowledgments

In the Name of Allah, the Most Gracious, the Most Merciful

All praise is due to Allah, who has guided us to this work.

I would like to express my deepest gratitude and sincere appreciation to my supervisor, **Dr. ABDELKEBIR Saad**, for his invaluable guidance, continuous support, patience, and encouragement throughout this research. His insightful advice and constructive feedback have been instrumental in shaping this work.

I am also deeply grateful to the members of the jury for their time, effort, and valuable evaluation of this dissertation. My sincere thanks go to:

- **Dr. FERAHTIA Nassim**, President of the jury, for his kindness and for presiding over the defense committee.
- **Dr. BENMEDDOUR Mohamed Ourabah**, Examiner, for his careful reading and insightful comments on this work.

My sincere thanks go to all my professors in the Department of Mathematics, University of Mohamed Boudiaf - M'sila, for their teachings and support throughout my academic journey.

I extend my heartfelt gratitude to my family, especially my parents, for their unwavering support, love, and encouragement. Without their sacrifices, this work would not have been possible.

Special thanks to my friends and colleagues for their moral support and encouragement.

LAMRI Ouarda

June 2026

Dedication

To my parents

Who taught me the value of knowledge and patience.

To my family and friends

For their love, support, and encouragement.

LAMRI Ouarda

Contents

List of Figures

List of Tables

List of Symbols

Greek Letters

α	Order of the fractional/fractal derivative, $\alpha \in (0, 1]$
$\Gamma(\cdot)$	Euler's Gamma function
λ	Constant parameter, often used in exponential functions or eigenvalues

Operators and Derivatives

${}_a^C D_+^\alpha$	Left Caputo fractional derivative of order α
${}_b^C D_-^\alpha$	Right Caputo fractional derivative of order α
$C^\alpha(\cdot)$	Chen–Hausdorff derivative of order α
$\mathcal{D}^\alpha(\cdot)$	New fractal derivative of order α
$I_\alpha(\cdot)$	Fractal integral of order α
${}^y\mathcal{D}^\alpha(\cdot)$	Yang derivative with respect to a function

Laplace Transforms

$\mathcal{L}\{\cdot\}(s)$	Classical Laplace transform
$\mathcal{L}_\alpha\{\cdot\}(s)$	Fractal Laplace transform of order α
$\mathcal{L}_\alpha^{-1}\{\cdot\}(t)$	Fractal inverse Laplace transform
$\mathcal{F}_\alpha(s)$	Notation for the fractal Laplace transform, $\mathcal{L}_\alpha\{f(t)\}(s)$

Polynomials and Special Functions

$P_n(x)$	Classical Legendre polynomial of degree n on $[-1, 1]$
$P_n^*(x)$	Shifted Legendre polynomial of degree n on $[0, 1]$

Numerical Methods

h	Step size in numerical methods (e.g., Runge-Kutta)
k_i	Increments used in the Runge-Kutta 4 (RK4) method

Sets and Variables

$\mathbb{R}$	Set of real numbers
$\mathbb{N}$	Set of natural numbers
u_0	Initial condition for the differential equation, $u(0) = u_0$

Introduction

Fractional calculus, a natural generalization of classical calculus, has emerged as a powerful mathematical tool for modeling complex phenomena in various fields of science and engineering. Unlike traditional integer-order derivatives, fractional operators incorporate memory and hereditary properties of materials and processes, making them particularly suitable for describing anomalous diffusion, viscoelastic materials, signal processing, and biological systems. The foundations of this theory were established in the seminal works of Oldham and Spanier [20], Samko, Kilbas and Marichev [23], and later developed extensively by Podlubny [21] and Kilbas et al. [15]. The non-local nature of fractional operators allows for a more accurate representation of real-world phenomena where the future state depends on the entire history of the system.

In recent years, a new branch of mathematics has gained significant attention: fractal calculus and fractal-fractional calculus. This emerging field combines concepts from fractal geometry with fractional calculus to describe processes occurring on fractal media or exhibiting fractal characteristics. The concept of Hausdorff derivatives was introduced by Chen [11] to describe anomalous diffusion phenomena, leading to the development of what is now known as Hausdorff calculus [17]. Subsequent research by Chen and his collaborators [13, 12, 8, 18] demonstrated the effectiveness of this approach in modeling complex systems exhibiting power-law and stretched exponential behaviors. More recently, Atangana [5] established a formal connection between fractal calculus and fractional calculus, introducing the concept of fractal-fractional differentiation and integration. The introduction of fractal derivatives provides a powerful framework for modeling phenomena in porous media, rough surfaces, and complex geometrical structures where traditional calculus falls short.

This master's thesis focuses on the study and analysis of time-fractal fractional differential equations, aiming to develop both analytical and numerical approaches for their solutions. The work is structured around a newly defined fractal derivative, which extends the classical derivative by incorporating a fractal time scale through transformations involving exponential functions, drawing inspiration from the work of Yang [24] on general calculi with respect to other functions.

In the first chapter, we present the fundamental mathematical concepts required throughout this work. We begin by recalling the definition of the Caputo fractional derivative, both left and right-sided,

as presented in standard references [21, 15, 7], which serves as a reference point for our investigations. The Chen-Hausdorff derivative [11, 13] is then introduced as a bridge between classical and fractal approaches. The core of this chapter is dedicated to defining a new fractal derivative of order $\alpha \in (0, 1]$, inspired by the work of Yang [24], where we establish its fundamental properties including linearity, product and quotient rules, and the chain rule. We also prove the continuity of α-differentiable functions and introduce the associated fractal integral, demonstrating the inverse relationship between the fractal derivative and its integral. These preliminary results form the theoretical foundation upon which the subsequent chapters are built.

In the second chapter, we develop analytical methods for solving fractal fractional differential equations. After reviewing the classical Laplace transform, we introduce its fractal counterpart and establish its fundamental properties. A key result presented in this chapter is the theorem linking the fractal Laplace transform of the derivative to the transform of the function itself. We provide a comprehensive table of fractal Laplace transforms for elementary functions, including exponentials, trigonometric functions, and polynomials. Using this framework, we solve several initial value problems involving the fractal derivative, demonstrating how the fractal Laplace transform converts these equations into algebraic equations in the transform domain. Through various illustrative examples, we obtain exact solutions that reveal the rich structure of fractal dynamics, including behaviors similar to those observed in Hausdorff dynamical systems [14, 12], and these exact solutions serve as benchmarks for the numerical methods developed later.

In the third chapter, we turn our attention to numerical approximation techniques, recognizing that many fractal fractional equations cannot be solved analytically. We focus on the classical fourth-order Runge-Kutta method, adapting it to handle fractal derivatives by first transforming the fractal equation into an equivalent ordinary differential equation. Through a series of numerical experiments, we compare the approximate solutions obtained via this method with the exact solutions from the previous chapter. The results demonstrate excellent agreement, with absolute errors remaining remarkably small throughout the computational domain. We provide tables of numerical values at discrete points to quantify the accuracy, and graphical comparisons illustrate the convergence and stability of the method for various values of the fractal order α.

In the fourth chapter, we extend our investigation to more sophisticated approximation techniques, specifically spectral methods based on orthogonal polynomials. We introduce classical Legendre polynomials on the interval $[-1, 1]$ and their shifted counterparts on $[0, 1]$, following the detailed study presented in [1]. A key theoretical contribution of this chapter is the derivation of a formula for expressing the fractal derivative of a function approximated by shifted Legendre polynomials.

This result, presented with detailed proof, allows for the discretization of time-fractal fractional equations into algebraic systems. We provide examples illustrating the application of this technique and compare the results with both exact solutions and Runge-Kutta approximations. The spectral method demonstrates high accuracy with relatively few terms, showcasing its potential for efficient numerical simulation of fractal systems.

Through this work, we aim to introduce and systematically study a new fractal derivative with well-defined properties, develop a complete analytical framework using the fractal Laplace transform, implement and validate numerical methods adapted to fractal equations, and apply spectral methods using shifted Legendre polynomials to fractal problems. The comprehensive set of examples and numerical experiments presented throughout this thesis demonstrates the effectiveness of the proposed approaches and their potential applications in physics, engineering, and applied mathematics, building upon the rich theoretical foundations established in the fields of fractional calculus and fractal analysis [20, 11, 17, 5, 23, 21, 15, 24].

Chapter 1

Basic concepts

This chapter presents the main mathematical notions that will be used throughout this work. We recall the definition of the Caputo fractional derivative and introduce the Chen–Hausdorff derivative. Then, we define a new fractal derivative and study its fundamental properties, including linearity, product and quotient rules, and the chain rule. Finally, we present the associated fractal integral and establish its basic relationship with the new derivative. These preliminary results form the theoretical foundation for the subsequent chapters.

1.1 Fractional derivatives of Caputo

Definition 1.1. [7] Let $\alpha > 0$, and $n = [\alpha] + 1$. The left Caputo fractional derivative of order α of f is defined by:

$$\forall t \in [a, b], \quad {}^{C}_{a}D^{\alpha}_{+} f(t) = \frac{1}{\Gamma(n-\alpha)} \int_a^t (t-\tau)^{n-\alpha-1} f^{(n)}(\tau)\, d\tau.$$

We also define its analogous to the right.

Definition 1.2. Let $\alpha > 0$, and $n = [\alpha] + 1$. The right Caputo fractional derivative of order α of f is defined by:

$$\forall t \in [a, b], \quad {}^{C}_{b}D^{\alpha}_{-} f(t) = \frac{(-1)^n}{\Gamma(n-\alpha)} \int_t^b (\tau-t)^{n-\alpha-1} f^{(n)}(\tau)\, d\tau.$$

1.2 The Chen Hausdorff derivative

Definition 1.3. The Chen Hausdorff derivative of the function [11, 13] $x(t)$ is defined as:

$$C^{\alpha}(x)(t) = \lim_{z \to t} \frac{x(z) - x(t)}{z^{\alpha} - t^{\alpha}}, \tag{1.1}$$

if x is differentiable, then

$$C^{\alpha}(x)(t) = \frac{t^{1-\alpha}}{\alpha} x'(t). \tag{1.2}$$

This definition is crucial for our work as it links fractal calculus to classical differentiation, enabling the modeling of complex phenomena such as anomalous diffusion and porous media. Throughout

this research, we will adopt this derivative as our main tool for analyzing fractal fractional differential equations.

Theorem 1.1 (Properties of the Chen-Hausdorff derivative [19])**.** *Let f and g be α-differentiable functions, and let $\lambda \in \mathbb{R}$ be a constant. Then the following properties hold:*

1. ***Linearity:***
$$C^\alpha(af + bg) = aC^\alpha(f) + bC^\alpha(g), \qquad \forall a, b \in \mathbb{R}.$$
2. ***Derivative of a constant:***
$$C^\alpha(\lambda) = 0.$$
3. ***Product rule:***
$$C^\alpha(fg)(t) = C^\alpha(f)(t)\, g(t) + f(t)\, C^\alpha(g)(t).$$
4. ***Quotient rule:***
$$C^\alpha\left(\frac{f}{g}\right)(t) = \frac{C^\alpha(f)(t)\, g(t) - C^\alpha(g)(t)\, f(t)}{g^2(t)}, \qquad g(t) \neq 0.$$
5. ***Chain rule:***
$$C^\alpha(f \circ g)(t) = f'(g(t))\, C^\alpha(g)(t).$$

Proof. Parts (1) and (2) follow directly from the definition.

$$\begin{aligned} C^\alpha(f+g)(t) &= \lim_{z\to t} \frac{(af+bg)(z) - (af+bg)(t)}{z^\alpha - t^\alpha} \\ &= a \lim_{z\to t} \frac{(f)(z) - (f)(t)}{z^\alpha - t^\alpha} + b \lim_{z\to t} \frac{(g)(z) - (g)(t)}{z^\alpha - t^\alpha} \\ &= aC^\alpha(f) + bC^\alpha(g). \end{aligned}$$

For (3):

$$\begin{aligned} C^\alpha(fg)(t) &= \lim_{z\to t} \frac{f(z)g(z) - f(t)g(t)}{z^\alpha - t^\alpha} \\ &= C^\alpha(f)(t)g(t) + C^\alpha(g)(t)f(t). \end{aligned}$$

For (4):

$$C^\alpha\left(\frac{f}{g}\right)(t) = \frac{C^\alpha(f)(t)g(t) - C^\alpha(g)(t)f(t)}{g^2(t)}.$$

For (5):We have

$$\begin{aligned} C^\alpha(f \circ g)(t) &= \lim_{z\to t} \frac{f(g(z)) - f(g(t))}{z^\alpha - t^\alpha} \\ &= \lim_{z\to t} \frac{f(g(z)) - f(g(t))}{g(z) - g(t)} \cdot \frac{g(z) - g(t)}{z^\alpha - t^\alpha} \\ &= f'(g(t))\, C^\alpha(g)(t). \end{aligned}$$

□

1.3 New fractal derivative

Definition 1.4. [24] Let a function $x : I \subset \mathbb{R} \longrightarrow \mathbb{R}$. Then the fractal derivative $\mathcal{D}^\alpha$ of x of order $\alpha \in (0, 1)$ is defined by:

$$\mathcal{D}^\alpha(x)(t) = \lim_{h \to t} \frac{x(h) - x(t)}{e^{h^\alpha} - e^{t^\alpha}}. \tag{1.3}$$

We say x is α-differentiable if $F_x^\alpha(t)$ exist for all $t \in I$.

if x differentiable , then

$$\mathcal{D}^\alpha(x)(t) = \frac{t^{1-\alpha}}{\alpha e^{t^\alpha}} x'(t) \tag{1.4}$$

proof We have

$$\begin{aligned}
\mathcal{D}^\alpha(x)(t) &= \lim_{h \to t} \frac{x(h) - x(t)}{e^{h^\alpha} - e^{t^\alpha}} \\
&= \lim_{h \to t} \frac{x(h) - x(t)}{h - t} \lim_{h \to t} \frac{h - t}{e^{h^\alpha} - e^{t^\alpha}} \\
&= x'(t) \frac{1}{\lim_{h \to t} \frac{e^{h^\alpha} - e^{t^\alpha}}{h - t}}, \text{use of Hospital's Theorem} \\
&= \frac{t^{1-\alpha}}{\alpha e^{t^\alpha}} x'(t).
\end{aligned}$$

or,

Direct use of L′Hospital′s .

Proposition 1.1. The definition 1.3 rewards The definition 1.4.

Proof. Assume that x is differentiable and

$$C^\alpha(x)(t) = \frac{t^{1-\alpha}}{\alpha} x'(t).$$

From the relation

$$\mathcal{D}^\alpha(x)(t) = e^{-t^\alpha} C^\alpha(x)(t),$$

we obtain

$$\mathcal{D}^\alpha(x)(t) = e^{-t^\alpha} \left(\frac{t^{1-\alpha}}{\alpha} x'(t) \right).$$

Hence,

$$\boxed{\mathcal{D}^\alpha(x)(t) = \frac{t^{1-\alpha}}{\alpha e^{t^\alpha}} x'(t)}.$$

□

Properties 1.1. The fractal derivative of order α satisfies the following properties for elementary functions:

1. $\mathcal{D}^{\alpha}(1) = 0$.
2. $\mathcal{D}^{\alpha}(t^{p}) = p\, t^{p-\alpha}$.
3. $\mathcal{D}^{\alpha}\left(e^{t^{\alpha}}\right) = 1$.
4. $\mathcal{D}^{\alpha}\left(e^{e^{t^{\alpha}}}\right) = e^{e^{t^{\alpha}}}$.
5. $\mathcal{D}^{\alpha}\left(e^{\lambda e^{t^{\alpha}}}\right) = \lambda\, e^{\lambda e^{t^{\alpha}}}$.

Remark 1.1. Let x α-differentiable, if $\alpha = 1$, then x is differentiable.

Theorem 1.2. *If a function $x : I \subset \mathbb{R} \longrightarrow \mathbb{R}$ is α-differentiable at t_0, $\alpha \in (0, 1)$, then x is continuous at t_0.*

proof Since

$$x(h) - x(t_0) = \frac{x(h) - x(t_0)}{e^{h^{\alpha}} - e^{t_0^{\alpha}}}(e^{h^{\alpha}} - e^{t_0^{\alpha}}).$$

Then,

$$\lim_{h \to t_0}[x(h) - x(t_0)] = \lim_{h \to t_0} \frac{x(h) - x(t_0)}{e^{h^{\alpha}} - e^{t_0^{\alpha}}} \lim_{h \to t_0}(e^{h^{\alpha}} - e^{t_0^{\alpha}}),$$

so

$$\lim_{h \to t_0}[x(h) - x(t_0)] = \mathcal{D}^{\alpha}(x)(t_0),$$

which implies that $\lim_{h \to t_0} x(h) = x(t_0)$, hence, x is continuous at t_0.

The $\mathcal{D}^{\alpha}$ satisfies all the properties in the following theorem.

Theorem 1.3. *Let f and g are α-differentiable. We have,*

1. $\mathcal{D}^{\alpha}(af + bg) = a\mathcal{D}^{\alpha}(f) + b\mathcal{D}^{\alpha}(g)$, *for all* $a, b \in \mathbb{R}$.
2. $\mathcal{D}^{\alpha}(\lambda) = 0$, *for all constant functions* $f(x) = \lambda$.
3. $\mathcal{D}^{\alpha}(fg)(t) = \mathcal{D}^{\alpha}(f)(t)g(t) + f(t)\mathcal{D}^{\alpha}(g)(t)$.
4. $\mathcal{D}^{\alpha}\left(\frac{f}{g}\right)(t) = \frac{\mathcal{D}^{\alpha}(f)(t)g(t) - \mathcal{D}^{\alpha}(g)(t)f(t)}{g^{2}(t)}$, $for\ g(t) \neq 0$.

Proof. Parts (1) through (2) in theorem 1.3 follow directly from the definition.

$$\begin{aligned}\mathcal{D}^\alpha(f+g)(t) &= \lim_{h\to t}\frac{(f+g)(h)-(f+g)(t)}{e^{h^\alpha}-e^{t^\alpha}}\\ &= \lim_{h\to t}\frac{f(h)+g(h)-f(t)-g(t)}{e^{h^\alpha}-e^{t^\alpha}}\\ &= \lim_{h\to t}\frac{f(h)-f(t)}{e^{h^\alpha}-e^{t^\alpha}}+\lim_{h\to t}\frac{g(h)-g(t))}{e^{h^\alpha}-e^{t^\alpha}}\\ &= \mathcal{D}^\alpha(f)+\mathcal{D}^\alpha(g).\end{aligned}$$

in (2), for $f(h)=\lambda$ and $f(t)=\lambda$,

$$\mathcal{D}^\alpha(\lambda)=\lim_{h\to t}\frac{f(h)-f(t)}{e^{h^\alpha}-e^{t^\alpha}}=0.$$

For (3): Now, for fixed t,

$$\begin{aligned}\mathcal{D}^\alpha(fg)(t) &= \lim_{h\to t}\frac{f(h)g(h)-f(t)g(t)}{e^{h^\alpha}-e^{t^\alpha}}\\ &= \lim_{h\to t}\frac{f(h)g(h)-f(t)g(h)+f(t)g(h)-f(t)g(t)}{e^{h^\alpha}-e^{t^\alpha}}\\ &= \lim_{h\to t}\frac{(f(h)-f(t))g(h)}{e^{h^\alpha}-e^{t^\alpha}}+\lim_{h\to t}\frac{f(t)(g(h)-g(t))}{e^{h^\alpha}-e^{t^\alpha}}\\ &= \mathcal{D}^\alpha(f)(t)g(t)+\mathcal{D}^\alpha(g)(t)f(t).\end{aligned}$$

For (4): Now, for fixed t,

$$\begin{aligned}\mathcal{D}^\alpha\left(\frac{f}{g}\right)(t) &= \lim_{h\to t}\frac{\frac{f(h)}{g(h)}-\frac{f(t)}{g(t)}}{e^{h^\alpha}-e^{t^\alpha}}\\ &= \lim_{h\to t}\frac{f(h)g(t)-f(t)g(h)}{g(h)g(t)(e^{h^\alpha}-e^{t^\alpha})}\\ &= \lim_{h\to t}\frac{f(h)g(t)-f(t)g(t)+f(t)g(t)-f(t)g(h)}{g(h)g(t)(e^{h^\alpha}-e^{t^\alpha})}\\ &= \lim_{h\to t}\frac{f(h)-f(t)}{e^{h^\alpha}-e^{t^\alpha}}\frac{g(t)}{g(h)g(t)}-\lim_{h\to t}\frac{f(t)(g(h)-g(t))}{g(h)g(t)(e^{h^\alpha}-e^{t^\alpha})}\\ &= \frac{\mathcal{D}^\alpha(f)(t)g(t)-\mathcal{D}^\alpha(g)(t)f(t)}{g^2(t)},\end{aligned}$$

since f and g are α-differentiable.

$$\mathcal{D}^\alpha\left(\frac{f}{g}\right)(t)=\frac{\mathcal{D}^\alpha(f)(t)\frac{g(t)}{g(t)g(t)}-\frac{f(t)}{g(t)}\mathcal{D}^\alpha(g)(t)}{g(t)^2}=\frac{\mathcal{D}^\alpha(f)(t)g(t)-\mathcal{D}^\alpha(g)(t)f(t)}{g(t)^2}.$$

□

Theorem 1.4 (Fractal chain rule)**.** *Let f differentiable and g α-differentiable. We have,*

$$\mathcal{D}^\alpha(f\circ g)(t)=f'(g(t))\mathcal{D}^\alpha(g)(t).$$

Proof.

$$\begin{aligned}\mathcal{D}^{\alpha}(f\circ g)(t) &= \lim_{h\to 0}\frac{f(g(h))-f(g(t))}{h^{\alpha}-t^{\alpha}}\\ &= \lim_{h\to t}\frac{f(g(h))-f(g(t))}{g(h)-g(t)}\,\frac{g(h)-g(t)}{h^{\alpha}-t^{\alpha}}\\ &= f'(g(t))\mathcal{D}^{\alpha}(g)(t).\end{aligned}$$

□

1.4 Fractional YANG derivative

YANG in [24] generalized derivative with respect to another function is defined:

$${}^{y}\mathcal{D}^{\alpha}(y)(t) = \frac{1}{H'(t)}x'(t), \quad H'(t) > 0.$$

Remark 1.2. 1. If $\alpha = 1$, the YANG derivative ${}^{y}\mathcal{D}^{\alpha}$ and new fractal derivative $\mathcal{D}^{\alpha}$ coincide.

2. If $H(t) = e^{e^{t^{\alpha}}}$,then

$$\mathcal{D}^{\alpha}(x)(t) = {}^{y}\mathcal{D}^{\alpha}(x)(t)$$

1.5 Fractal integral

When it comes to integration, the most important class of functions to define the integral is the space of continuous functions.

Definition 1.5 ([19])**.** Let $\alpha \in (0,1]$ and let $f : [0,+\infty) \to \mathbb{R}$ be a continuous function. The Hausdorff fractional integral of order α is defined by

$$I_{\alpha}(f)(t) = \int_0^t \alpha s^{\alpha-1} f(s)\, ds, \quad t \geq 0.$$

Definition 1.6 ([4])**.** by 1.4 Let $\alpha \in (0,1]$,

$$I_{\alpha}(f)(t) = \int_0^t \alpha s^{\alpha-1} e^{s^{\alpha}} f(s) ds.$$

One of the nice results is the following.

Theorem 1.5. *for t, where f is any continuous function in the domain of I_{α}.*

$$\mathcal{D}^{\alpha} I_{\alpha}(f)(t) = f(t).$$

Proof. Since f is continuous, then $I_\alpha(f)(t)$ is clearly differentiable.

Hence,

$$\begin{aligned}\mathcal{D}^\alpha\big(I_\alpha(f)\big)(t) &= \frac{1}{\alpha t^{\alpha-1}e^{t^\alpha}}\frac{d}{dt}I_\alpha(f)(t)\\ &= \frac{1}{\alpha t^{\alpha-1}e^{t^\alpha}}\frac{d}{dt}\int_0^t \alpha s^{\alpha-1}e^{s^\alpha}f(s)\,ds\\ &= \frac{1}{\alpha t^{\alpha-1}e^{t^\alpha}}\alpha t^{\alpha-1}e^{t^\alpha}f(t)\\ &= f(t).\end{aligned}$$

Theorem 1.6. *Let $f:\mathbb{R}\to\mathbb{R}$ be differentiable and $0<\alpha\le 1$. Then,*

$$I_\alpha\big(\mathcal{D}^\alpha(f)\big)(t) = f(t) - f(0).$$

proof We have

$$\begin{aligned}I_\alpha\big(\mathcal{D}^\alpha(f)\big)(t) &= \int_0^t \alpha s^{\alpha-1}e^{s^\alpha}\mathcal{D}^\alpha(f)(s)\,ds\\ &= \int_0^t \alpha s^{\alpha-1}e^{s^\alpha}\frac{1}{\alpha s^{\alpha-1}e^{s^\alpha}}f'(s)\,ds\\ &= \int_0^t f'(s)\,ds\\ &= f(t)-f(0).\end{aligned}$$

Remark 1.3. We say $\mathcal{D}^\alpha\big(I_\alpha(f)\big)(t) = I_\alpha\big(\mathcal{D}^\alpha(f)\big)(t)$ if $f(0)=0$.

1.6 The Cauchy Problem for Fractal Fractional Differential Equations

1.6.1 Classical Cauchy Problem

Definition 1.7 ([2])**.** Let $I\subset\mathbb{R}$ be an interval, $t_0\in I$, and $y_0\in\mathbb{R}^n$. Let

$$f: I\times\mathbb{R}^n\to\mathbb{R}^n$$

be a given function.

The **Cauchy problem** (or initial value problem) consists of finding a function

$$y: I\to\mathbb{R}^n$$

such that

$$\begin{cases} y'(t) = f(t,y(t)), & t\in I,\\ y(t_0)=y_0.\end{cases}$$

If f is continuous in a neighborhood of (t_0,y_0), we look for a solution $y\in C^1(I)$.

Theorem 1.7 (Picard–Lindelöf Theorem [2]). *Let $I \subset \mathbb{R}$ be an interval containing t_0, and let*

$$f : I \times \mathbb{R}^n \to \mathbb{R}^n$$

be continuous on a region $\Omega \subset I \cdot \mathbb{R}^n$ containing (t_0, y_0).

Suppose that f satisfies a local Lipschitz condition *with respect to y on Ω, i.e., there exists a constant $L > 0$ such that*

$$\|f(t, y_1) - f(t, y_2)\| \leq L \|y_1 - y_2\|$$

for all $(t, y_1), (t, y_2) \in \Omega$.

Then there exist an interval $J \subset I$ with $t_0 \in J$ and a unique function

$$y \in C^1(J, \mathbb{R}^n)$$

such that

$$\begin{cases} y'(t) = f(t, y(t)), & t \in J, \\ y(t_0) = y_0. \end{cases}$$

1.6.2 Fractal Cauchy Problem

In this work, we are interested in the following **fractal Cauchy problem** involving the fractal derivative $\mathcal{D}^\alpha$ defined in the previous section:

$$\begin{cases} \mathcal{D}^\alpha u(t) = u(t) + f(t), & t > 0,\ \alpha \in (0, 1], \\ u(0) = u_0, \end{cases} \tag{1.5}$$

where $\mathcal{D}^\alpha$ is the fractal derivative operator, $f(t)$ is a given source term, and u_0 is the initial condition.

Using the relationship between the fractal derivative and the classical derivative:

$$\mathcal{D}^\alpha u(t) = \frac{t^{1-\alpha}}{\alpha} u'(t),$$

the fractal Cauchy problem can be transformed into an equivalent classical initial value problem:

$$\begin{cases} u'(t) = \frac{\alpha e^{t^\alpha}}{t^{1-\alpha}} \big(u(t) + f(t)\big), & t > 0, \\ u(0) = u_0. \end{cases} \tag{1.6}$$

This formulation allows us to apply classical analytical and numerical methods, such as the fractal Laplace transform and Runge-Kutta schemes, to obtain exact and approximate solutions for fractal fractional differential equations.

Chapter 2

Exact Solutions of Fractal Fractional Differential Equations Using the Fractal Laplace Transform

We investigate fractional differential equations involving the fractional fractal derivative using both analytical and numerical approaches. First, we introduce the definition of the Laplace transform associated with the fractional fractal derivative, based on reference [A], and employ it to obtain exact solutions for several fractional fractal differential equations.

2.1 Classical Laplace Transform

Definition 2.1. [16]If f is a function (locally integrable), defined on $\mathbb{R}_+$, with values in $\mathbb{C}$, we call the classical Laplace transform of f the function

$$\mathcal{L}\{f\}(s) = \int_0^{+\infty} e^{-st} f(t)\, dt = \lim_{x\to+\infty} \int_0^x e^{-st} f(t)\, dt, \tag{2.1}$$

for the values of s for which this integral converges.

2.2 The fractal Laplace transform

Definition 2.2. [24]Let $0 < \alpha \leq 1$ and $f : \mathbb{R} \to \mathbb{R}$ be a real valued function. Then the fractal Laplace transform of order α of f is defined by:

$$\mathcal{L}_\alpha\{f(t)\}(s) = \mathcal{F}_\alpha(s) = \alpha \int_0^\infty e^{-st^\alpha} f(t)\, t^{\alpha-1} e^{t^\alpha}\, dt.$$

Theorem 2.1. *Let $0 < \alpha \leq 1$ and $f : \mathbb{R} \to \mathbb{R}$ be a differentiable real valued function. Then,*

$$\mathcal{L}_\alpha\big(\mathcal{D}^\alpha(f)(t)\big)(s) = s\mathcal{F}_\alpha(s) - e^{-s} f(0).$$

proof We have

$$\begin{aligned}
\mathcal{L}_\alpha\{\mathcal{D}^\alpha(f)(t)\}(s) &= \alpha \int_0^\infty e^{-se^{t^\alpha}} \mathcal{D}^\alpha(f)(t)\, t^{\alpha-1} e^{t^\alpha}\, dt \\
&= \alpha \int_0^\infty e^{-se^{t^\alpha}} \frac{1}{\alpha t^{\alpha-1} e^{t^\alpha}} f'(t)\, t^{\alpha-1} e^{t^\alpha}\, dt \\
&= \int_0^\infty e^{-se^{t^\alpha}} f'(t)\, dt \\
&= \left[e^{-se^{t^\alpha}} f(t)\right]_0^\infty - \alpha s \int_0^\infty e^{-se^{t^\alpha}} f(t)\, t^{\alpha-1} e^{t^\alpha}\, dt \\
&= -e^{-s} f(0) + sD_\alpha(s).
\end{aligned}$$

Lemme 2.1. *Let $f : \mathbb{R} \to \mathbb{R}$ be a function such that $L_\alpha\{f(t)\}(s) = \mathcal{D}_\alpha(s)$ exists. Then*

$$\mathcal{F}_\alpha(s) = \mathcal{L}\left\{f\left((\log t)^{1/\alpha}\right)\right\}(s),$$

where

$$\mathcal{L}\{g(t)\}(s) = \int_1^\infty e^{-st} g(t)\, dt.$$

Proof.

The proof follows by the change of variable $u = e^{t^\alpha}$. Then

$$\begin{cases} t \to 0 \;\Rightarrow\; u \to 1, \\ t \to \infty \;\Rightarrow\; u \to \infty. \end{cases}$$

From $u = e^{t^\alpha}$, we get

$$t = (\log u)^{\frac{1}{\alpha}}.$$

Differentiating, we obtain

$$du = \alpha t^{\alpha-1} e^{t^\alpha} dt = \alpha t^{\alpha-1} u\, dt,$$

which gives

$$dt = \frac{1}{\alpha} (\log u)^{\frac{1}{\alpha}-1} \frac{1}{u}\, du.$$

Substituting into the definition of the transform, we obtain

$$L_\alpha\{f(t)\}(s) = \int_0^\infty e^{-se^{t^\alpha}} f(t)\, \alpha t^{\alpha-1} e^{t^\alpha} dt.$$

Using the change of variable, this becomes

$$L_\alpha\{f(t)\}(s) = \int_1^\infty e^{-su} f\left((\log u)^{\frac{1}{\alpha}}\right) du.$$

Hence,

$$\mathcal{D}_\alpha(s) = \mathcal{L}\left\{f\left((\log t)^{1/\alpha}\right)\right\}(s).$$

□

Proposition 2.1. 1. If the functions f and g are transformable, then there is the transform of the sum and is equal to the sum of the transforms, that is:

$$L_\alpha\{f+g\} = L_\alpha\{f\} + L_\alpha\{g\}$$

2. If the function f is transformable and λ is a real number, then there is the transform of product ofλ by$f$ and is equal to product of$\lambda$by the transform of f , that is:

$$L_\alpha\{\lambda f\} = \lambda L_\alpha\{f\}$$

proof Taking into account the two previous propositions, we say that L_α is a linear operator.
The following table summarizes the most important and commonly used fractal Laplace transforms for functions depending on t^α. These results are essential for solving fractal fractional differential equations analytically.

Function $f(t)$	**Fractal Laplace Transform** $\mathcal{L}_\alpha\{f(t)\}(s)$
1	$\dfrac{e^{-s}}{s}, \quad s>0$
$e^{-ae^{t^\alpha}}$	$\dfrac{e^{-(s+a)}}{s+a}, \quad s>-a$
e^{t^α}	$e^{-s}\left(\dfrac{1}{s}+\dfrac{1}{s^2}\right), \quad s>0$
$e^{-e^{t^\alpha}}$	$\dfrac{e^{-(s+1)}}{s+1}, \quad s>-1$
$\sin(t^\alpha)$	$\displaystyle\int_0^\infty e^{-se^x}\, e^x \sin(x)\, dx$
$\cos(t^\alpha)$	$\displaystyle\int_0^\infty e^{-se^x}\, e^x \cos(x)\, dx$

Table 2.1: Table of Fractal Laplace Transforms.

This table clearly displays the fractal Laplace transforms of various elementary functions, showing their explicit dependence on the fractal order α through the argument t^α. These transforms will be used throughout this chapter to obtain exact solutions of fractal fractional differential equations.

Proof From definition directly.

2.3 Fractal Inverse Laplace Transform

The fractal inverse Laplace transform is an extension of the classical inverse Laplace transform, applicable to functions and systems described by *fractional-order derivatives* of order $\alpha \in (0,1]$. Let $F(s)$ denote the Laplace transform of a fractal function $f(t)$, defined for $t \geq 0$. The fractal inverse Laplace transform, denoted by $\mathcal{L}_\alpha^{-1}$, is the operator that reconstructs $f(t)$ in the time domain while

accounting for the non-integer derivative order:

$$f(t) = \mathcal{L}_\alpha^{-1}\{F(s)\}.$$

In the context of a fractal differential equation:

$$\mathcal{D}^\alpha f(t) = g(t), \qquad f^{(k)}(0^+) = f_k, \quad k = 0, \ldots, n-1, \quad n-1 < \alpha \leq n,$$

where $\mathcal{D}^\alpha$ denotes the fractal (or fractional) derivative of order α, the Laplace transform [22] of $\mathcal{D}^\alpha f(t)$ is given by:

$$\mathcal{L}\{\mathcal{D}^\alpha f(t)\} = s^\alpha F(s) - \sum_{k=0}^{n-1} s^{\alpha-1-k} f^{(k)}(0^+).$$

The time-domain solution $f(t)$ is often expressed using the *Mittag -Leffler function* $E_\alpha(z)$, which generalizes the exponential function to fractional systems [3]:

$$f(t) = \sum_{k=0}^{\infty} \frac{(\lambda t^\alpha)^k}{\Gamma(\alpha k + 1)}, \qquad \text{for } F(s) = \frac{s^{\alpha-1}}{s^\alpha - \lambda}.$$

This approach provides a rigorous framework for solving fractional differential equations and analyzing systems exhibiting memory effects or fractal dynamics, which cannot be captured by classical integer-order models.

2.4 Problem Formulation

In this section, we take the problem for fractional differential equation of order α, given by

$$\begin{cases} \mathcal{D}^\alpha u(t) = u(t) + f(t), & \alpha \in]0, 1], \\ u(0) = u_0 \end{cases} . \tag{2.2}$$

In order to solve problem (2.2), we transform it into an equivalent problem involving a classical derivative by relying on (1.3) related to the fractional fractal derivative. Consequently, the fractional fractal differential equation is reduced to an ordinary differential equation with a classical derivative

2.4.1 Exact solutions using the fractal Laplace transform

In this section, the fractal Laplace transform was used as the main tool to solve fractional differential equations, whether ordinary equations or linear systems, while taking into account the fractal order α. The method is based on first transforming the fractional differential equation into an algebraic equation in the fractal Laplace space, then solving this equation to obtain the function $\mathcal{D}_\alpha(s)$, and finally returning to the time domain using the inverse fractal Laplace transform to obtain an explicit solution that depends on α.

Example 2.1. Consider the fractal initial value problem:

$$\begin{cases} \mathcal{D}^{\alpha} y(t) = \lambda y(t), & t \geq 0, \\ y(0) = y_0 = 1. \end{cases} \tag{2.3}$$

Applying the fractal Laplace Transform to both sides of equation (2.3), we get

$$L_{\alpha}\mathcal{D}^{\alpha} y(t) = L_{\alpha}\lambda y(t)(s)$$

by Theorem 2.1 ,we have

$$L_{\alpha}\mathcal{D}^{\alpha}(t) = s\mathcal{D}_{\alpha}(s) - e^{-s}y(0) \tag{2.4}$$

$$= sD_{\alpha}(s) - e^{-s}y_0 \tag{2.5}$$

and by Proposition 2.2

$$L_{\alpha}\lambda y(t)(s) = \lambda\mathcal{D}_{\alpha}(s) \tag{2.6}$$

hence

$$\begin{aligned} \mathcal{D}_{\alpha}(s) &= \frac{e^{-s}}{s-\lambda} y_0 \\ &= \frac{e^{\lambda - s}}{s-\lambda} e^{\lambda} y_0. \end{aligned}$$

We using the inverse fractal Laplace transform and table 2.1

$$\begin{aligned} L_{\alpha}^{-1}\mathcal{D}_{\alpha}(s)(t) &= L_{\alpha}^{-1}\left(\frac{e^{\lambda - s}}{s-\lambda}\right)(s) e^{\lambda} y_0 \\ &= e^{\lambda e^{t^{\alpha}}} e^{-\lambda} y_0. \end{aligned}$$

the exact solution of example 2.2 is $y(t) = e^{\lambda e^{t^{\alpha}}} e^{-\lambda} y_0$.

Example 2.2. Consider the fractal initial value problem:

$$\begin{cases} \mathcal{D}^{\alpha} y(t) = y(t) + 1, & t \geq 0, \\ y(0) = y_0 = 0. \end{cases} \tag{2.7}$$

Applying the fractal Laplace Transform to both sides of equation 2.3, we get

$$L_{\alpha}\mathcal{D}^{\alpha} y(t) = L_{\alpha} y(t)(s),$$

by theorem 2.1 ,we have

$$L_{\alpha}\mathcal{D}^{\alpha} y(t) = s\mathcal{D}_{\alpha}(s) - e^{-s}y(0) \tag{2.8}$$

$$= sD_{\alpha}(s) - e^{-s}y_0 \tag{2.9}$$

and by proposition 2.2

$$L_\alpha(y(t)+1)(s) = \mathcal{D}_\alpha(s) + \frac{e^{-s}}{s} \tag{2.10}$$

hence

$$\begin{aligned}\mathcal{D}_\alpha(s) &= \frac{e^{-s}}{s(s-1)} \\ &= -\frac{e^{-s}}{s} + \frac{e^{-s}}{s-1}.\end{aligned}$$

We using the inverse fractal Laplace transform and table 2.1

$$\begin{aligned}L_\alpha^{-1}\mathcal{D}_\alpha(s)(t) &= L_\alpha^{-1}(-\frac{e^{-s}}{s})(s) + L_\alpha^{-1}(\frac{e^{-s}}{s-1})(s) \\ &= e^{e^{t^\alpha}}e^{-1} - 1.\end{aligned}$$

the exact solution of example 2.2 is $y(t) = e^{e^{t^\alpha}}e^{-1} - 1$.

Example 2.3. Consider the fractal initial value problem:

$$\begin{cases} \mathcal{D}^\alpha y(t) = e^{\alpha t}, \quad t \geq 0, \\ y(0) = 0. \end{cases} \tag{2.11}$$

Applying the fractal Laplace Transform to both sides of equation 2.3, we get

$$L_\alpha\mathcal{D}^\alpha(t) = L_\alpha(e^{\alpha t})$$

by Theorem 2.1 ,we have

$$L_\alpha\mathcal{D}^\alpha(t) = s\mathcal{D}_\alpha(s) - e^{-s}y(0) \tag{2.12}$$

$$= sD_\alpha(s) \tag{2.13}$$

and by proposition 2.2

$$L_\alpha e^{\alpha t} = \frac{1}{s-1} \tag{2.14}$$

hence

$$\begin{aligned}sD_\alpha(s) &= \frac{1}{s-1} \\ D_\alpha(s) &= -\frac{1}{s} + \frac{1}{s-1}.\end{aligned}$$

We using the inverse fractal Laplace transform and table 2.1

$$L_\alpha^{-1}(\mathcal{D}_\alpha(s))(t) = L_\alpha^{-1}(-\frac{1}{s}) + L_\alpha^{-1}(\frac{1}{s-1})$$
$$= e^{t^\alpha} - 1,$$

the exact solution of example 2.3 is $y(t) = e^{t^\alpha} - 1$.

Example 2.4. Consider the initial value problem

$$\begin{cases} \mathcal{D}^\alpha u(t) = u(t) - tcos(t) + \frac{t^{1-\alpha}}{\alpha}(cos(t) - tsin(t)), & \alpha \in]0,1], \\ u(0) = 0. \end{cases} \tag{2.15}$$

The exact solution for this problem is $u(t) = tcos(t)$.

Proof Verification of exact solution example 3.10

Consider the fractional initial value problem

$$D^\alpha u(t) = u(t) - t\cos(t) + \frac{t^{1-\alpha}}{\alpha}\big(\cos(t) - t\sin(t)\big) \tag{2.16}$$

Using the Chen–Hausdorff definition

$$\mathcal{D}^\alpha u(t) = \frac{1}{\alpha} t^{1-\alpha} u'(t),$$

we obtain

$$\frac{1}{\alpha} t^{1-\alpha} u'(t) = u(t) - t\cos(t) + \frac{t^{1-\alpha}}{\alpha}(\cos(t) - t\sin(t)).$$

Multiplying by $\alpha t^{\alpha-1}$, we get

$$u'(t) = \alpha t^{\alpha-1} u(t) - \alpha t^\alpha \cos(t) + \cos(t) - t\sin(t).$$

Rewriting,

$$u'(t) - \alpha t^{\alpha-1} u(t) = -\alpha t^\alpha \cos(t) + \cos(t) - t\sin(t).$$

The integrating factor is

$$\mu(t) = e^{-t^\alpha}.$$

Then

$$\frac{d}{dt}\big(u(t)e^{-t^\alpha}\big) = e^{-t^\alpha}\big(-\alpha t^\alpha \cos(t) + \cos(t) - t\sin(t)\big).$$

Since

$$\frac{d}{dt}(t\cos(t)) = \cos(t) - t\sin(t),$$

we obtain

$$\frac{d}{dt}\left(u(t)e^{-t^{\alpha}}\right) = \frac{d}{dt}\left(t\cos(t)\,e^{-t^{\alpha}}\right).$$

Hence

$$u(t)e^{-t^{\alpha}} = t\cos(t)\,e^{-t^{\alpha}} + C,$$

so

$$u(t) = t\cos(t) + Ce^{t^{\alpha}}.$$

Using $u(0) = 0$, we get $C = 0$, hence

$$u(t) = t\cos(t).$$

Since both sides coincide and the assumed function satisfies the equation, the function $u(t) = t\cos(t)$ is the exact solution.

Example 2.5. Consider the initial value problem

$$\begin{cases} \mathcal{D}^{\alpha}u(t) = u(t) - te^{-t} + \frac{t^{1-\alpha}}{\alpha}e^{-t}(1-t), & \alpha \in]0,1], \\ u(0) = 0 \end{cases} . \tag{2.17}$$

The exact solution for this problem is $u(t) = te^{-t}$.

Verification of exact solution for Example 3.8.

Consider the fractional initial value problem

$$D^{\alpha}u(t) = u(t) - te^{-t} + \frac{t^{1-\alpha}}{\alpha}e^{-t}(1-t), \qquad u(0) = 0. \tag{2.18}$$

Using the Chen–Hausdorff definition

$$\mathcal{D}^{\alpha}u(t) = \frac{1}{\alpha}t^{1-\alpha}u'(t),$$

we obtain

$$\frac{1}{\alpha}t^{1-\alpha}u'(t) = u(t) - te^{-t} + \frac{t^{1-\alpha}}{\alpha}e^{-t}(1-t).$$

Multiplying both sides by $\alpha t^{\alpha-1}$, we get

$$u'(t) = \alpha t^{\alpha-1}u(t) - \alpha t^{\alpha}e^{-t} + e^{-t}(1-t).$$

Rewriting, we obtain the linear equation

$$u'(t) - \alpha t^{\alpha-1}u(t) = -\alpha t^{\alpha}e^{-t} + e^{-t}(1-t).$$

The integrating factor is

$$\mu(t) = e^{-t^\alpha}.$$

Multiplying the equation by $\mu(t)$, we get

$$\frac{d}{dt}\big(u(t)e^{-t^\alpha}\big) = e^{-t^\alpha}\big(-\alpha t^\alpha e^{-t} + e^{-t}(1-t)\big).$$

Since

$$\frac{d}{dt}(te^{-t}) = e^{-t}(1-t),$$

we deduce that

$$\frac{d}{dt}\big(u(t)e^{-t^\alpha}\big) = \frac{d}{dt}\big(te^{-t}\, e^{-t^\alpha}\big).$$

Integrating both sides yields

$$u(t)e^{-t^\alpha} = te^{-t}\, e^{-t^\alpha} + C.$$

Thus,

$$u(t) = te^{-t} + Ce^{t^\alpha}.$$

Using the initial condition $u(0) = 0$, we obtain $C = 0$. Therefore,

$$u(t) = te^{-t}.$$

Hence, the exact solution is $u(t) = te^{-t}$.

Example 2.6. Consder the initial value problem

$$\begin{cases} \mathcal{D}^\alpha u(t) = u(t) - sin(t) - \frac{t^{1-\alpha}}{\alpha} cos(t), & \alpha \in]0,1], \\ u(0) = 0 \end{cases} . \tag{2.19}$$

The exact solution for this problem is u(t)=sin(t).

Proof Verification of exact solution for Example 2.19.

Consider the fractional initial value problem

$$D^\alpha u(t) = u(t) - \sin(t) - \frac{t^{1-\alpha}}{\alpha}\cos(t), \qquad u(0) = 0. \tag{2.20}$$

Using the Chen–Hausdorff definition

$$\mathcal{D}^\alpha u(t) = \frac{1}{\alpha} t^{1-\alpha} u'(t),$$

we obtain

$$\frac{1}{\alpha} t^{1-\alpha} u'(t) = u(t) - \sin(t) - \frac{t^{1-\alpha}}{\alpha}\cos(t).$$

Multiplying both sides by $\alpha t^{\alpha-1}$, we get

$$u'(t) = \alpha t^{\alpha-1}u(t) - \alpha t^{\alpha}\sin(t) - \cos(t).$$

Rewriting,

$$u'(t) - \alpha t^{\alpha-1}u(t) = -\alpha t^{\alpha}\sin(t) - \cos(t).$$

The integrating factor is

$$\mu(t) = e^{-t^{\alpha}}.$$

Multiplying by $\mu(t)$,

$$\frac{d}{dt}\big(u(t)e^{-t^{\alpha}}\big) = e^{-t^{\alpha}}\big(-\alpha t^{\alpha}\sin(t) - \cos(t)\big).$$

Since

$$\frac{d}{dt}(\sin(t)) = \cos(t),$$

we deduce that

$$\frac{d}{dt}\big(u(t)e^{-t^{\alpha}}\big) = \frac{d}{dt}\big(\sin(t)\, e^{-t^{\alpha}}\big).$$

Integrating,

$$u(t)e^{-t^{\alpha}} = \sin(t)\, e^{-t^{\alpha}} + C.$$

Thus,

$$u(t) = \sin(t) + Ce^{t^{\alpha}}.$$

Using $u(0) = 0$, we obtain $C = 0$. Hence,

$$u(t) = \sin(t).$$

Example 2.7. Consider the initial value problem

$$\begin{cases} \mathcal{D}^{\alpha}u(t) = u(t) - t^2 + \frac{t^{1-\alpha}}{\alpha}2t, & \alpha \in]0,1], \\ u(0) = 0 \end{cases} . \tag{2.21}$$

The exact solution for this problem is ,$u(t) = t^2$

Proof Proof

Verification of exact solution for Example 2.21.

Consider the fractional initial value problem

$$D^{\alpha}u(t) = u(t) - t^2 + \frac{t^{1-\alpha}}{\alpha}2t, \qquad u(0) = 0. \tag{2.22}$$

Using the Chen–Hausdorff definition

$$\mathcal{D}^{\alpha}u(t) = \frac{1}{\alpha}t^{1-\alpha}u'(t),$$

we obtain

$$\frac{1}{\alpha}t^{1-\alpha}u'(t) = u(t) - t^2 + \frac{t^{1-\alpha}}{\alpha}2t.$$

Multiplying both sides by $\alpha t^{\alpha-1}$, we get

$$u'(t) = \alpha t^{\alpha-1}u(t) - \alpha t^{\alpha}t^2 + 2t.$$

Rewriting,

$$u'(t) - \alpha t^{\alpha-1}u(t) = -\alpha t^{\alpha+2} + 2t.$$

The integrating factor is

$$\mu(t) = e^{-t^{\alpha}}.$$

Multiplying,

$$\frac{d}{dt}\big(u(t)e^{-t^{\alpha}}\big) = e^{-t^{\alpha}}\big(-\alpha t^{\alpha+2} + 2t\big).$$

Since

$$\frac{d}{dt}(t^2) = 2t,$$

we obtain

$$\frac{d}{dt}\big(u(t)e^{-t^{\alpha}}\big) = \frac{d}{dt}\big(t^2\, e^{-t^{\alpha}}\big).$$

Integrating,

$$u(t)e^{-t^{\alpha}} = t^2\, e^{-t^{\alpha}} + C.$$

Thus,

$$u(t) = t^2 + Ce^{t^{\alpha}}.$$

Using $u(0) = 0$, we get $C = 0$. Hence,

$$u(t) = t^2.$$

Chapter 3

Approximate solutions of fractal fractional equations

On this chapter, we focus on constructing approximate solutions for fractal fractional differential equations through the application of the classical fourth-order Runge–Kutta method (RK4).

3.1 Approximate solution of deformable fractional equation by Rang-Kutta-4 method

3.1.1 Fourth Order Runge-Kutta Method (RK4)

This method was investigated by two German mathematicians, Runge around 1894 and later extended by Kutta [10]. It is one of the most important numerical methods known as the Runge-Kutta method, which allows us to obtain greater accuracy at each step while requiring only an initial value of $y(x)$ together with the differential equation.

The Fourth Order Runge-Kutta Method is most commonly used in all engineering applications. It is broadly used for solving initial value problems (IVP) for ordinary differential equations (ODEs).

General Formula

Consider the initial value problem

$$\begin{cases} \frac{dy}{dx} = f(x, y), \\ y(x_0) = y_0, \end{cases} \tag{3.1}$$

and let the step size be h. Define:

$$\begin{aligned} k_1 &= hf(x_0, y_0), \\ k_2 &= hf\Big(x_0 + \frac{h}{2},\ y_0 + \frac{k_1}{2}\Big), \\ k_3 &= hf\Big(x_0 + \frac{h}{2},\ y_0 + \frac{k_2}{2}\Big), \\ k_4 &= hf(x_0 + h,\ y_0 + k_3). \end{aligned}$$

Then the next value is computed as:

$$y_{n+1} = y_n + \frac{1}{6}\big(k_1 + 2k_2 + 2k_3 + k_4\big), \quad n = 0, 1, 2, 3, \ldots \tag{3.2}$$

RK4 Procedure

1. Identify $f(x, y)$, x_0, y_0, and the step size h.
2. Compute k_1, k_2, k_3, k_4 using the formulas above.
3. Update y_{n+1} using the weighted sum of k values.
4. Repeat the process for the required number of steps.

3.1.2 Numerical solution of example

Figure shows the comparison between the numerical solution obtained by the fourth-order Runge–Kutta (RK4) method and the exact solution. The left plot illustrates the excellent agreement between both solutions, confirming the high accuracy of RK4. The right plot presents the absolute error, which remains very small over the whole interval, demonstrating the stability and convergence of the method.

Example 3.1. Consider the following fractal Cauchy problem with the initial condition,

$$\begin{cases} \mathcal{D}^{\alpha} u(t) = u(t) + 1, \quad \alpha \in (0, 1], \\ u(0) = 0. \end{cases} \tag{3.3}$$

The exact solution for this problem, derived using the fractal Laplace transform [4, 3], is:

$$u(t) = e^{e^{t^{\alpha}} - 1} - 1. \tag{3.4}$$

The equivalent standard differential problem is obtained by applying the definition $\mathcal{D}^{\alpha}(u)(t) = \frac{t^{1-\alpha}}{\alpha e^{t^{\alpha}}} u'(t)$ [5, 4]:

$$\begin{cases} u'(t) = \frac{\alpha e^{t^{\alpha}}}{t^{1-\alpha}}(u(t) + 1), \quad \alpha \in (0, 1], \\ u(0) = 0. \end{cases} \tag{3.5}$$

The table presents a numerical comparison between the approximate solution computed using the fourth-order Runge-Kutta (RK4) method and the exact solution at different points of the interval. We observe a strong agreement between the two values at all nodes, as the absolute error remains relatively small and gradually decreases as we move along the domain. This behavior indicates the high accuracy and numerical stability of the method, and confirms its ability to provide a reliable approximation of the true solution even with a moderate step size. The results also suggest that the method possesses the convergence property, which is consistent with the theoretical fourth-order accuracy of the RK4 method.

The time t	Exact solution	Approximate solution	Absolute error
0.0000	0.0000	0.0000	0.0000
0.2000	0.4660	0.4655	0.0005
0.4000	0.9970	0.9965	0.0005
0.6000	1.7510	1.7500	0.0010
0.8000	2.8640	2.8625	0.0015
1.0000	4.5745	4.5730	0.0015

Table 3.1: Comparison between RK4 numerical solution and exact solution with absolute error for N=5 ($\alpha = 0.7$).

The time t	Exact solution	Approximate solution	Absolute error
0.0000	0.0000	0.0000	0.0000
0.1000	0.2284	0.2281	0.0003
0.2000	0.4660	0.4655	0.0005
0.3000	0.7173	0.7168	0.0005
0.4000	0.9970	0.9965	0.0005
0.5000	1.3170	1.3163	0.0007
0.6000	1.7510	1.7500	0.0010
0.7000	2.2300	2.2287	0.0013
0.8000	2.8640	2.8625	0.0015
0.9000	3.6400	3.6380	0.0020
1.0000	4.5745	4.5730	0.0015

Table 3.2: Comparison between RK4 numerical solution and exact solution with absolute error for N=10 ($\alpha = 0.7$).

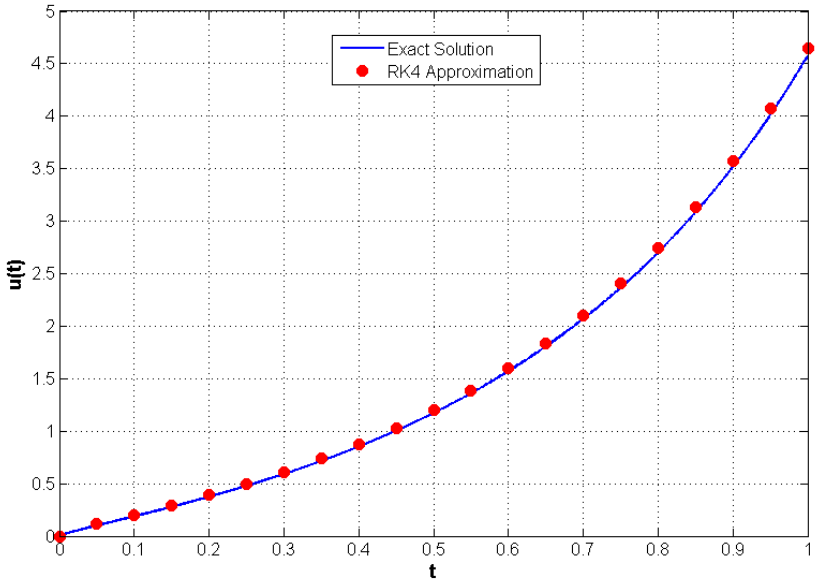

Figure 3.1: Comparison of the numerical and exact solutions of the example 3.3 for $\alpha = 0.7$

Example 3.2. Consider the initial value problem

$$\begin{cases} C^{\alpha}u(t) = u(t) - tcos(t) + \frac{t^{1-\alpha}}{\alpha}(cos(t) - tsin(t)), & \alpha \in]0, 1], \\ u(0) = 1 \end{cases} . \tag{3.6}$$

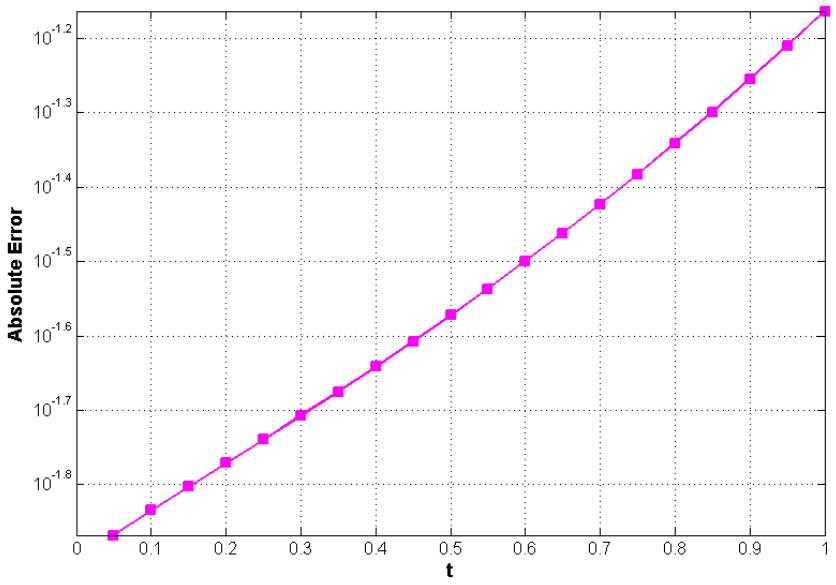

Figure 3.2: Absolute error between the numerical and exact solutions for example 3.3 for $\alpha = 0.7$

The exact solution for this problem is $u(t) = tcos(t)$.

The equivalent problem for 3.6 is as follows

$$\begin{cases} u'(t) = \frac{\alpha}{t^{1-\alpha}}(u(t) - tcos(t)) + cos(t) - tsin(t), & \alpha \in]0, 1], \\ u(0) = 1. \end{cases} \tag{3.7}$$

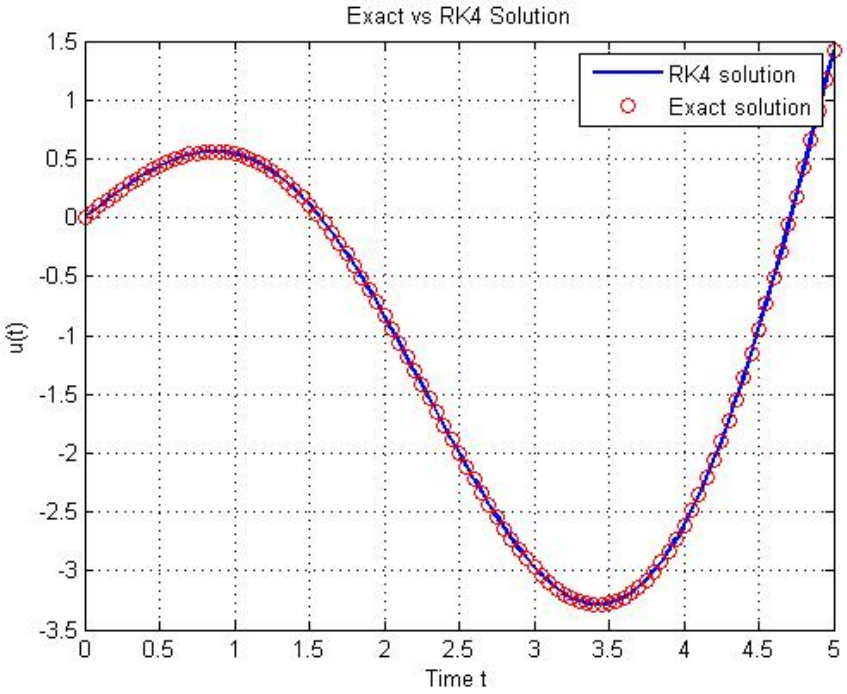

Figure 3.3: Comparison of the numerical and exact solutions of the example 3.6 for $\alpha = 0.6$

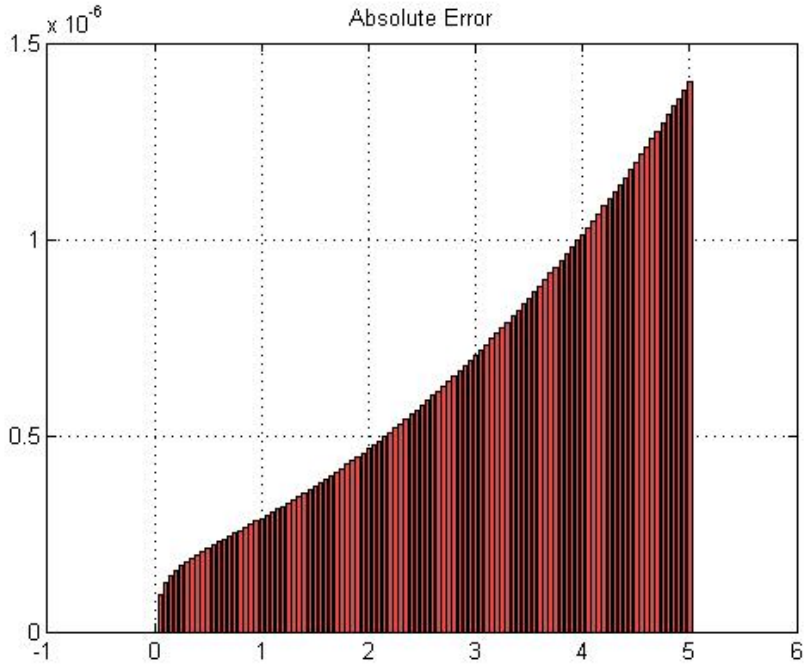

Figure 3.4: Absolute error between the numerical and exact solutions for example 3.6 with $\alpha = 0.6$.

Example 3.3. Consider the initial value problem

$$\begin{cases} C^{\alpha}u(t) = u(t) - te^{-t} + \frac{t^{1-\alpha}}{\alpha}e^{-t}(1-t), & \alpha \in]0,1], \\ u(0) = 0 \end{cases} . \tag{3.8}$$

The exact solution for this problem is $u(t) = te^{-t}$.

The equivalent problem for 3.8 is as follows

$$\begin{cases} u'(t) = \frac{\alpha}{t^{1-\alpha}}(u(t) - te^{-t}) + e^{-t}(1-t), & \alpha \in]0,1], \\ u(0) = 0. \end{cases} \tag{3.9}$$

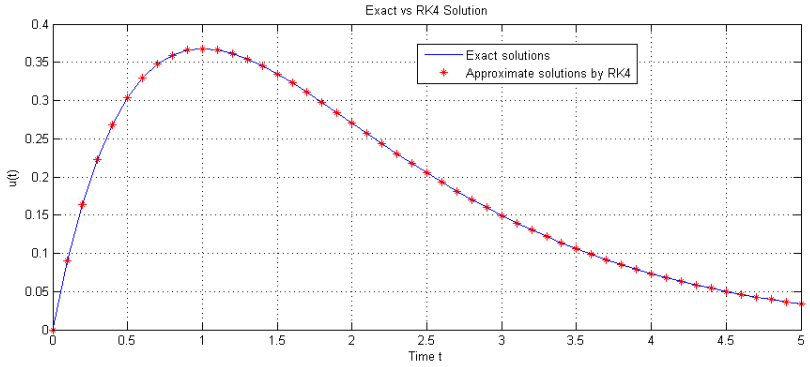

Figure 3.5: Comparison of the numerical and exact solutions of the example 3.8 for $\alpha = 0.8$

Example 3.4. Consder the initial value problem

$$\begin{cases} C^{\alpha}u(t) = u(t) - sin(t) - \frac{t^{1-\alpha}}{\alpha}cos(t), & \alpha \in]0,1], \\ u(0) = 0 \end{cases} . \tag{3.10}$$

The exact solution for this problem is u(t)=sin(t).

The equivalent problem for 3.10 is as follows

$$\begin{cases} u'(t) = \frac{\alpha}{t^{1-\alpha}}(u(t) - sin(t)) - cos(t), & \alpha \in]0, 1], \\ u(0) = 0. \end{cases} \tag{3.11}$$

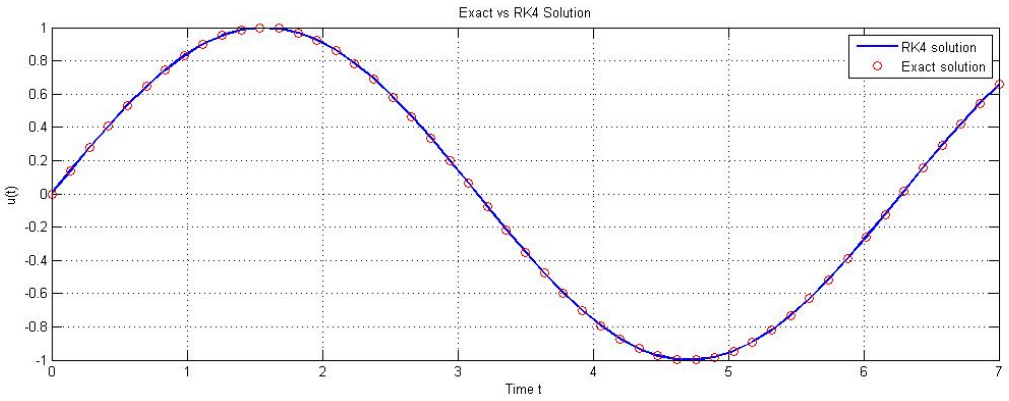

Figure 3.6: Comparison of the numerical and exact solutions of the example 3.10 for $\alpha = 0.8$

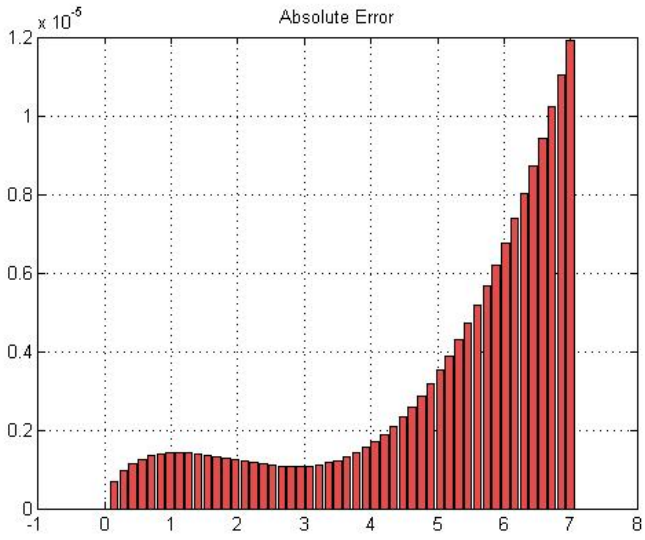

Figure 3.7: Absolute error between the numerical and exact solutions for example 3.10 for $\alpha = 0.8$

Example 3.5. Consider the initial value problem

$$\begin{cases} C^{\alpha}u(t) = u(t) - t^2 + \frac{t^{1-\alpha}}{\alpha}2t, & \alpha \in]0,1], \\ u(0) = 0 \end{cases} . \tag{3.12}$$

The exact solution for this problem is ,$u(t) = t^2$. The equivalent problem for 3.12 is as follows

$$\begin{cases} u'(t) = \frac{\alpha}{t^{1-\alpha}}(u(t) - t^2) + 2t, & \alpha \in]0,1], \\ u(0) = 0. \end{cases} \tag{3.13}$$

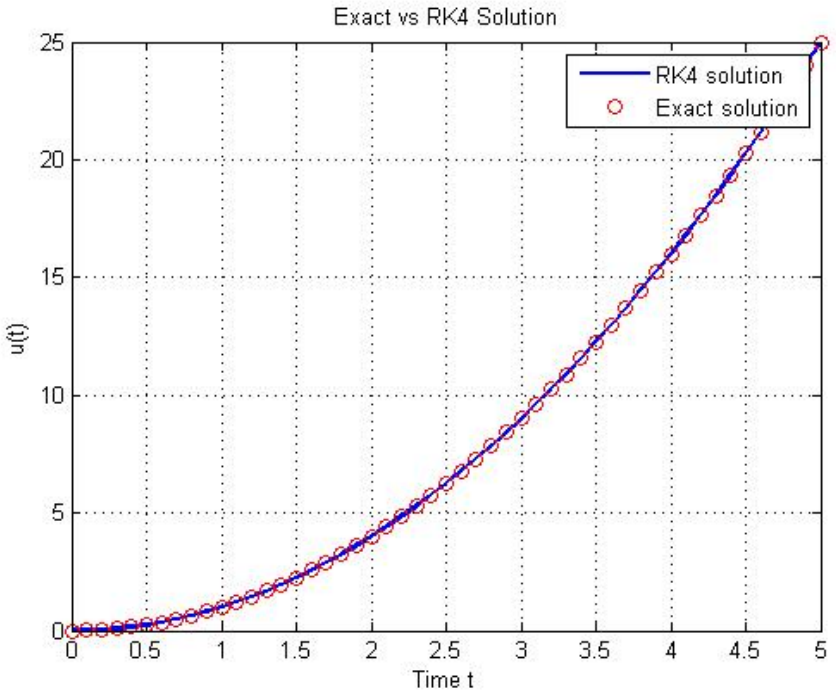

Figure 3.8: Comparison of the numerical and exact solutions of the example 3.12 for $\alpha = 0.85$

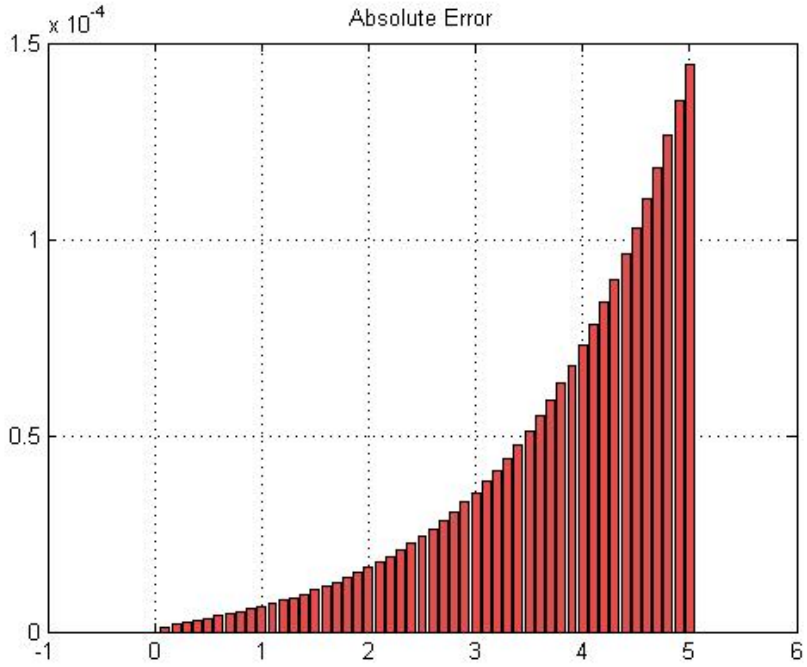

Figure 3.9: Comparison of the numerical and exact solutions of the example 3.12 for $\alpha = 0.85$

Chapter 4

Approximate Solutions of Time-Fractal Fractional Differential Equations

In Chapter 4, we focus on finding approximate solutions to time-fractal fractional differential equations. We combine spectral methods using Legendre polynomials (for spatial discretization) with classical numerical schemes like the Euler method (for time integration). Numerical examples with plots are presented to show the effectiveness of these methods.

4.1 Legendre Polynomials and Shifted Legendre Polynomials

4.1.1 Classical Legendre Polynomials

The classical Legendre polynomials $P_n(x)$ defined on the interval $[-1, 1]$ [9] are given by the following recurrence relation:

$$\begin{cases} P_0(x) = 1, \\ P_1(x) = x, \\ P_{i+1}(x) = \dfrac{2i+1}{i+1}\, x\, P_i(x) - \dfrac{i}{i+1} P_{i-1}(x), \quad i = 1, 2, 3, \ldots \end{cases} \tag{4.1}$$

The first few Legendre polynomials are:

$$\begin{aligned} P_0(x) &= 1, \\ P_1(x) &= x, \\ P_2(x) &= \frac{1}{2}(3x^2 - 1), \\ P_3(x) &= \frac{1}{2}(5x^3 - 3x), \\ P_4(x) &= \frac{1}{8}(35x^4 - 30x^2 + 3), \\ P_5(x) &= \frac{1}{8}(63x^5 - 70x^3 + 15x). \end{aligned} \tag{4.2}$$

4.1.2 Shifted Legendre Polynomials

For problems defined on the interval $[0, 1]$, it is convenient to use the shifted Legendre polynomials $P_i^*(x)$. These are obtained by applying the change of variable $z = 2x - 1$ (or equivalently $x = \frac{1}{2}(z+1)$) to the classical Legendre polynomials.

The shifted Legendre polynomials satisfy the following recurrence relation [20]:

$$\begin{cases} P_0^*(x) = 1, \\ P_1^*(x) = 2x - 1, \\ P_{i+1}^*(x) = \dfrac{(2i+1)(2x-1)}{i+1} P_i^*(x) - \dfrac{i}{i+1} P_{i-1}^*(x), \quad i = 1, 2, 3, \ldots \end{cases} \tag{4.3}$$

4.1.3 Explicit Analytical Form

The shifted Legendre polynomials can also be expressed in an explicit analytical form [20]:

$$P_i^*(x) = \sum_{k=0}^{i} (-1)^{i-k} \frac{\Gamma(i+k+1)}{\Gamma(i-k+1)\,[\Gamma(k+1)]^2}\, x^k, \quad i = 0, 1, 2, \ldots \tag{4.4}$$

where Γ denotes the Gamma function. This representation is particularly useful when computing fractal derivatives, as it expresses the polynomial as a linear combination of power functions.

The first few shifted Legendre polynomials obtained from this formula are:

$$\begin{aligned} P_0^*(x) &= 1, \\ P_1^*(x) &= 2x - 1, \\ P_2^*(x) &= 6x^2 - 6x + 1, \\ P_3^*(x) &= 20x^3 - 30x^2 + 12x - 1, \\ P_4^*(x) &= 70x^4 - 140x^3 + 90x^2 - 20x + 1, \\ P_5^*(x) &= 252x^5 - 630x^4 + 560x^3 - 210x^2 + 30x - 1. \end{aligned} \tag{4.5}$$

4.1.4 Orthogonality Property

The shifted Legendre polynomials satisfy the following orthogonality property on $[0, 1]$ [20]:

$$\int_0^1 P_i^*(x) P_j^*(x)\, dx = \begin{cases} \dfrac{1}{2i+1}, & \text{if } i = j \\ 0, & \text{if } i \neq j \end{cases} \tag{4.6}$$

This property is fundamental for series expansions, as it allows the efficient computation of the coefficients in a Legendre series.

4.1.5 Function Approximation Using Legendre Polynomials

A continuous function $g(x)$ defined on $[0, 1]$ can be approximated by a truncated Legendre series [9]:

$$g(x) \approx \sum_{i=0}^{N} c_i P_i^*(x) \tag{4.7}$$

where the coefficients c_i are given by the orthogonality property:

$$c_i = (2i + 1) \int_0^1 g(x) P_i^*(x)\, dx, \quad i = 0, 1, 2, \ldots, N \tag{4.8}$$

This approximation has the property that it minimizes the L^2 error for a given N, and for smooth functions, the coefficients decay rapidly, leading to high accuracy even with a small number of terms.

4.1.6 Rodrigues' Formula

Legendre polynomials can also be defined using Rodrigues' formula [6]:

$$P_n(x) = \frac{1}{2^n n!} \frac{d^n}{dx^n} \left((x^2 - 1)^n \right) \tag{4.9}$$

For shifted Legendre polynomials, the corresponding formula becomes:

$$P_n^*(x) = \frac{1}{2^n n!} \frac{d^n}{dx^n} \left((4x^2 - 4x)^n \right) \tag{4.10}$$

4.1.7 Useful Properties

Legendre polynomials possess several important properties that make them particularly suitable for spectral methods:

1. **Boundedness:** $|P_i^*(x)| \leq 1$ for all $x \in [0, 1]$

2. **Endpoint values:**

$$P_i^*(0) = (-1)^i, \quad P_i^*(1) = 1 \tag{4.11}$$

3. **Derivative recurrence:**

$$\frac{d}{dx} P_{i+1}^*(x) = (2i + 1) P_i^*(x) + \frac{d}{dx} P_{i-1}^*(x) \tag{4.12}$$

4. **Integral representation:**

$$P_i^*(x) = \frac{1}{\pi}\int_0^{\pi}\left[2x - 1 + 2i\sqrt{x - x^2}\cos\theta\right]^i d\theta \tag{4.13}$$

These properties, combined with the explicit form (4.4), make shifted Legendre polynomials an excellent choice for approximating solutions to fractal fractional differential equations, as they allow straightforward computation of fractal derivatives through term-by-term differentiation of the power series representation.

4.2 Problem Formulation

We consider the following time-fractal fractional diffusion equation:

$$\mathcal{D}_t^{(\alpha)}u(x,t) = \frac{\partial^2 u(x,t)}{\partial x^2} + f(x,t), \quad 0 \le x \le 1, \quad 0 \le t \le T \tag{4.14}$$

with:

- Initial condition: $u(x,0) = g(x)$, $0 \le x \le 1$
- Dirichlet boundary conditions: $u(0,t) = \varphi(t)$, $u(1,t) = \psi(t)$, $0 \le t \le T$

where:

☞ $0 < \alpha \le 1$ (order of the temporal fractal derivative)

☞ $\mathcal{D}_t^{(\alpha)}$ denotes the fractal derivative of order α with respect to t.

4.3 Evaluation of the Fractal Derivative Using Shifted Legendre Polynomials

One of the main advantages of using shifted Legendre polynomials is the ability to express their fractal derivatives in terms of power functions, which simplifies the numerical solution of fractal fractional differential equations.

Theorem 4.1. *Let $u_m(x)$ be an approximation of a function $u(x)$ expanded in terms of shifted Legendre polynomials as:*

$$u_m(x) = \sum_{i=0}^{m} c_i P_i^*(x) \tag{4.15}$$

where $P_i^*(x)$ is defined as in (4.4)*. Then, the second ordinary derivative of $u_m(x)$ can be expressed as:*

$$\frac{d^2u_m}{dx^2} = \sum_{i=2}^{m}\sum_{k=2}^{i} c_i Q_{i,k}\, x^{k-2} \tag{4.16}$$

where the coefficients $Q_{i,k}$ are given by:

$$Q_{i,k} = (-1)^{i-k}\frac{\Gamma(i+k+1)}{\Gamma(i-k+1)}\cdot\frac{k(k-1)}{[\Gamma(k+1)]^2} \tag{4.17}$$

or equivalently:

$$Q_{i,k} = (-1)^{i-k}\frac{\Gamma(i+k+1)}{\Gamma(i-k+1)\,\Gamma(k+1)\,\Gamma(k-1)}. \tag{4.18}$$

Proof. We begin by differentiating the series representation of $P_i^*(x)$ term by term. From (4.4), the first derivative is:

$$\frac{d}{dx}P_i^*(x) = \sum_{k=1}^{i}(-1)^{i-k}\frac{\Gamma(i+k+1)}{\Gamma(i-k+1)\,[\Gamma(k+1)]^2}\cdot k\,x^{k-1}. \tag{4.19}$$

Differentiating again:

$$\frac{d^2}{dx^2}P_i^*(x) = \sum_{k=2}^{i}(-1)^{i-k}\frac{\Gamma(i+k+1)}{\Gamma(i-k+1)\,[\Gamma(k+1)]^2}\cdot k(k-1)\,x^{k-2}. \tag{4.20}$$

Then:

$$\frac{d^2u_m}{dx^2} = \sum_{i=0}^{m} c_i\frac{d^2}{dx^2}P_i^*(x) = \sum_{i=2}^{m} c_i\sum_{k=2}^{i}(-1)^{i-k}\frac{\Gamma(i+k+1)}{\Gamma(i-k+1)\,[\Gamma(k+1)]^2}\cdot k(k-1)\,x^{k-2}. \tag{4.21}$$

Define $Q_{i,k}$ as in (4.17):

$$Q_{i,k} = (-1)^{i-k}\frac{\Gamma(i+k+1)}{\Gamma(i-k+1)}\cdot\frac{k(k-1)}{[\Gamma(k+1)]^2}. \tag{4.22}$$

Using $k(k-1) = \frac{\Gamma(k+1)}{\Gamma(k-1)}$, we get the equivalent form (4.18). Thus, (4.21) can be written as (4.18). □

4.4 Legendre Collocation Method for Time-Fractal Fractional Equations

We now apply the Legendre collocation method to solve problem (4.14) numerically.

We seek an approximate solution of the form:

$$u_m(x,t) = \sum_{i=0}^{m} c_i(t) P_i^*(x) \tag{4.23}$$

where $c_i(t)$ are unknown functions of time to be determined.

We substitute the approximation (4.23) into equation (4.14):

$$\sum_{i=0}^{m} \mathcal{D}_t^{(\alpha)}[c_i(t)] P_i^*(x) = \sum_{i=0}^{m} c_i(t) \frac{\partial^2 P_i^*(x)}{\partial x^2} + f(x,t). \tag{4.24}$$

Using the definition of the temporal fractal derivative for $0 < \alpha \leq 1$:

$$\mathcal{D}_t^{(\alpha)}[c_i(t)] = \frac{t^{1-\alpha}}{\alpha} c_i'(t) \tag{4.25}$$

Equation (4.24) becomes:

$$\sum_{i=0}^{m} \frac{t^{1-\alpha}}{\alpha} c_i'(t) P_i^*(x) = \sum_{i=2}^{m} \sum_{k=2}^{i} c_i(t) Q_{i,k} x^{k-2} + f(x,t) \tag{4.26}$$

We choose the collocation points x_p as the roots of the shifted Legendre polynomial $P_m^*(x)$, i.e.:

$$P_m^*(x_p) = 0, \quad p = 1, 2, \ldots, m \tag{4.27}$$

These points are well-known to provide excellent approximation properties.

Evaluating equation (4.26) at each collocation point x_p:

$$\sum_{i=0}^{m} \frac{t^{1-\alpha}}{\alpha} c_i'(t) P_i^*(x_p) - \sum_{i=2}^{m} \left[\sum_{k=2}^{i} Q_{i,k} x_p^{k-2} \right] c_i(t) = f(x_p, t), \quad p = 1, \ldots, m \tag{4.28}$$

4.4.1 Auxiliary Functions

For convenience, we define:

$$S_0(x_p) = S_1(x_p) = 0 \tag{4.29}$$

$$S_i(x_p) = \sum_{k=2}^{i} Q_{i,k} x_p^{k-2}, \quad i = 2, 3, \ldots, m. \tag{4.30}$$

Equation (4.28) can then be written as:

$$\sum_{i=0}^{m} \frac{t^{1-\alpha}}{\alpha} c_i'(t) P_i^*(x_p) - \sum_{i=0}^{m} S_i(x_p) c_i(t) = f(x_p, t), \quad p = 1, \ldots, m. \tag{4.31}$$

4.4.2 Boundary Conditions

Applying the boundary conditions to the approximation (4.23) and using the endpoint values (4.11):

$$u(0,t) = \sum_{i=0}^{m} c_i(t) P_i^*(0) = \sum_{i=0}^{m} c_i(t)(-1)^i = \varphi(t) \tag{4.32}$$

$$u(1,t) = \sum_{i=0}^{m} c_i(t) P_i^*(1) = \sum_{i=0}^{m} c_i(t) = \psi(t) \tag{4.33}$$

4.4.3 Matrix Formulation

Equations (4.31) (m equations) together with (4.32) and (4.33) (2 equations) form a system of $m + 2$ first-order ordinary differential equations for the unknown coefficients $c_i(t)$.

We write this system in matrix form:

$$A(t)X'(t) - BX(t) = F(t) \tag{4.34}$$

where:

- $X(t) = [c_0(t), c_1(t), \ldots, c_m(t)]^T$ is the vector of unknown coefficients
- $A(t)$ is an $(m + 1) \times (m + 1)$ matrix with entries $\frac{t^{1-\alpha}}{\alpha} P_i^*(x_p)$ for the first m rows, and zeros for the last two rows
- B is an $(m + 1) \times (m + 1)$ matrix that does not depend on time
- $F(t)$ is the source vector defined by:

$$F(t) = \begin{pmatrix} f(x_0, t) \\ f(x_1, t) \\ \vdots \\ f(x_{m-1}, t) \\ \varphi(t) \\ \psi(t) \end{pmatrix} \tag{4.35}$$

More explicitly:

$$A(t) = \frac{t^{1-\alpha}}{\alpha} \begin{pmatrix} P_0^*(x_0) & P_1^*(x_0) & \cdots & P_m^*(x_0) \\ P_0^*(x_1) & P_1^*(x_1) & \cdots & P_m^*(x_1) \\ \vdots & \vdots & \ddots & \vdots \\ P_0^*(x_{m-1}) & P_1^*(x_{m-1}) & \cdots & P_m^*(x_{m-1}) \\ 0 & 0 & \cdots & 0 \\ 0 & 0 & \cdots & 0 \end{pmatrix} \tag{4.36}$$

$$B = \begin{pmatrix} S_0(x_0) & S_1(x_0) & \cdots & S_m(x_0) \\ S_0(x_1) & S_1(x_1) & \cdots & S_m(x_1) \\ \vdots & \vdots & \ddots & \vdots \\ S_0(x_{m-1}) & S_1(x_{m-1}) & \cdots & S_m(x_{m-1}) \\ 1 & -1 & \cdots & (-1)^m \\ 1 & 1 & \cdots & 1 \end{pmatrix} \tag{4.37}$$

where $S_i(x_p)$ are defined as:

$$S_i(x_p) = \sum_{k=2}^{i} Q_{i,k} x_p^{k-2}, \quad i \geq 2 \tag{4.38}$$

and $S_0(x_p) = S_1(x_p) = 0$. The coefficients $Q_{i,k}$ are given by:

$$Q_{i,k} = (-1)^{i-k} \frac{\Gamma(i+k+1)}{\Gamma(i-k+1)} \cdot \frac{k(k-1)}{[\Gamma(k+1)]^2} \tag{4.39}$$

4.5 Numerical Solution Using Euler's Method

To solve the system of ODEs (4.34), we employ the forward Euler method.

4.5.1 Time Discretization

Divide the time interval $[0, T]$ into N equal steps of size $\tau = T/N$. Let $t_n = n\tau$ for $n = 0, 1, \ldots, N$, and denote:

$$X^n = X(t_n), \quad A^n = A(t_n), \quad F^n = F(t_n)$$

Note that B is constant in time.

4.5.2 Euler Approximation

Using the forward difference approximation for the derivative:

$$X'(t_n) \approx \frac{X^{n+1} - X^n}{\tau}$$

Substituting into (4.34) evaluated at t_n:

$$A^n \frac{X^{n+1} - X^n}{\tau} - BX^n = F^n$$

4.5.3 Recurrence Formula

Multiplying both sides by τ:

$$A^n(X^{n+1} - X^n) - \tau BX^n = \tau F^n$$

Rearranging terms:

$$A^n X^{n+1} = A^n X^n + \tau BX^n + \tau F^n$$

Solving for X^{n+1}:

$$X^{n+1} = X^n + \tau (A^n)^{-1}(BX^n + F^n)$$

Note that since A^n is not a square matrix, we use the pseudo-inverse:

$$X^{n+1} = X^n + \tau \operatorname{inv}(A^n)\,(BX^n + F^n).$$

4.5.4 Initial Condition

From the initial condition $u(x, 0) = g(x)$:

$$\sum_{i=0}^{m} c_i(0) P_i^*(x) = g(x) \tag{4.40}$$

Using the orthogonality property (4.6), the initial coefficients are given by:

$$c_i(0) = (2i + 1) \int_0^1 g(x) P_i^*(x)\, dx, \quad i = 0, 1, \ldots, m$$

4.6 Algorithm Summary

Algorithm 1 Euler's Method for Time-Fractal Fractional Equations

i. **Initialization:**

   a. Choose m (number of Legendre basis functions) and N (number of time steps).

   b. Compute time step $\tau = T/N$.

   c. Compute collocation points x_p (roots of $P_m^*(x)$), $p = 1, \ldots, m$.

   d. Compute matrix B using (4.37) and (4.38).

   e. Compute initial coefficient vector X^0 using (4.35).

ii. **Time Marching:**

   a. For $n = 0$ to $N - 1$:

      i. Compute $t_n = n\tau$.

      ii. Compute matrix $A^n = A(t_n)$ using (4.40).

      iii. Compute source vector $F^n = F(t_n)$.

      iv. Compute $X^{n+1} = X^n + \tau\,(A^n)^{-1}\,(BX^n + F^n)$.

iii. **Output:**

   a. Coefficients $c_i(t_n)$ for each time step.

   b. Approximate solution $u_m(x, t_n) = \sum_{i=0}^{m} c_i(t_n) P_i^*(x)$ at any desired x.

4.7 Numerical examples

In this part, we present some examples to illustrate the method and show that the algorithm works correctly and gives accurate numerical results.

Example 4.1. Consider the following time-fractional differential equation:

$$\begin{cases} \mathcal{D}_t^{(\alpha)} u(x,t) = \dfrac{\partial^2 u(x,t)}{\partial x^2} + f(x,t), \quad 0 \le x \le 1, \quad 0 \le t \le 1 \\ u(x,0) = 0, \quad 0 \le x \le 1 \\ u(0,t) = 0, \quad u(1,t) = 0, \quad 0 < t \le 1 \end{cases}$$

where $\alpha = 0.5$ is the fractional order parameter, and $\mathcal{D}_t^{(\alpha)}$ denotes the fractional derivative of order α.

The source term is given by:

$$f(x,t) = \frac{t^{1-\alpha}}{\alpha}(x - x^2) + 2t, \quad 0 < \alpha < 1$$

For $\alpha = 0.5$, this becomes:

$$f(x,t) = \frac{t^{0.5}}{0.5}(x - x^2) + 2t = 2t^{0.5}(x - x^2) + 2t$$

The exact solution of this problem is:

$$u_{\text{exact}}(x,t) = t(x - x^2)$$

We solve this problem using the Legendre collocation method with $m = 3$ (using shifted Legendre polynomials up to degree 3). The time interval $[0, 1]$ is divided into $N = 5$ time steps with step size $h = T/N = 0.2$.

The shifted Legendre polynomials used are:

$$P_1^*(x) = 2x - 1$$

$$P_2^*(x) = 6x^2 - 6x + 1$$

$$P_3^*(x) = 20x^3 - 30x^2 + 12x - 1$$

The numerical solution is approximated by:

$$u_{\text{num}}(x,t) = c_0(t) + c_1(t)P_1^*(x) + c_2(t)P_2^*(x) + c_3(t)P_3^*(x)$$

where the coefficients $c_0(t), c_1(t), c_2(t), c_3(t)$ are determined at each time step.

The collocation points x_0 and x_1 are chosen at the boundaries of the domain.

The matrices G and K are constructed as follows:

$$G = \frac{t^{1-\alpha}}{\alpha}\begin{pmatrix} 1 & P_1^*(x_0) & P_2^*(x_0) & P_3^*(x_0) \\ 1 & P_1^*(x_1) & P_2^*(x_1) & P_3^*(x_1) \\ 0 & 0 & 0 & 0 \\ 0 & 0 & 0 & 0 \end{pmatrix}$$

$$K = \begin{pmatrix} 1 & P_1^*(x_0) & P_2^*(x_0) + 12 & P_3^*(x_0) - 60 \\ 1 & P_1^*(x_1) & P_2^*(x_1) + 12 & P_3^*(x_1) - 60 + 120 \\ 1 & -1 & 1 & -1 \\ 1 & 1 & 1 & 1 \end{pmatrix}$$

The source vector is:

$$F = \begin{pmatrix} \frac{t^{1-\alpha}}{\alpha}(x_0 - x_0^2) + 2t \\ \frac{t^{1-\alpha}}{\alpha}(x_1 - x_1^2) + 2t \\ 0 \\ 0 \end{pmatrix}$$

At each time step, we solve the linear system:

$$(G - hK)V = GV_1 + hF$$

where V_1 contains the coefficients from the previous time step, and V contains the new coefficients $[c_0, c_1, c_2, c_3]^T$.

The numerical solution is then compared with the exact solution, and the errors are computed using:

$$L_2 \text{ error} = \sqrt{\int_0^1 (u_{\text{exact}} - u_{\text{num}})^2 \, dx}$$

$$L_\infty \text{ error} = \max_{0 \le x \le 1} |u_{\text{exact}} - u_{\text{num}}|$$

The figures (4.1)-(4.4) shows the exact and numerical solutions at different time steps, while Figures (4.6a),(4.6b) display 3D visualizations of both solutions and the error between them.

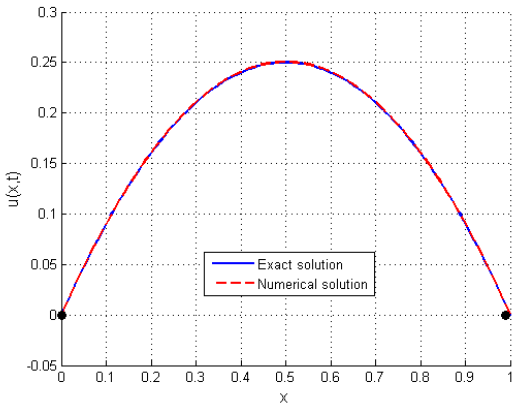

Figure 4.1: Planar representation of exact and approximate solutions for fractional order $\alpha = 0.75$ over $t = 1$

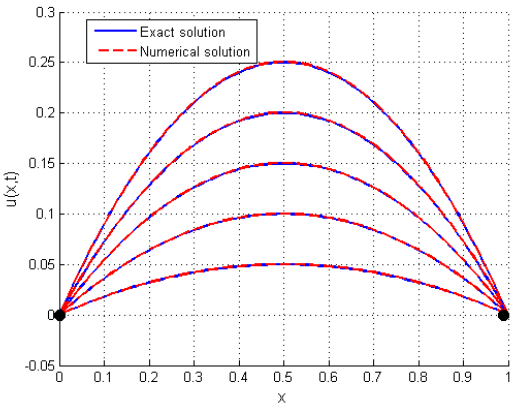

Figure 4.2: Planar representation of exact and approximate solutions for fractional order $\alpha = 0.8$ over $t = 0.2 - 0.4 - 0.6 - 0.8 - 1$

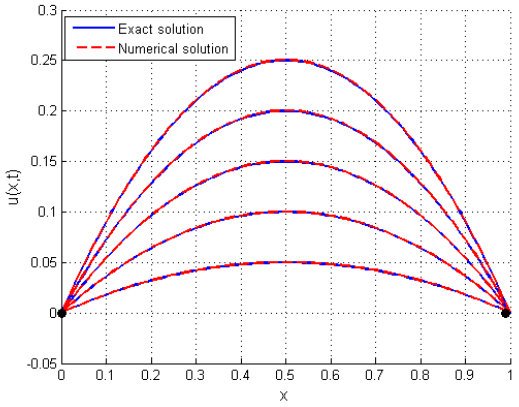

Figure 4.3: Planar representation of exact and approximate solutions for fractional order $\alpha = 0.5$ over $t = 0.2 - 0.4 - 0.6 - 0.8 - 1$

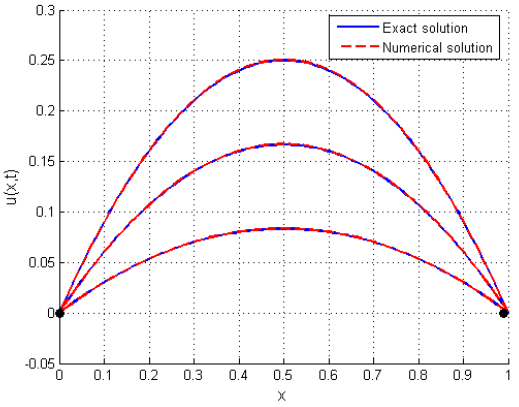

Figure 4.4: Planar representation of exact and approximate solutions for fractional order $\alpha = 0.8$ over $t = 0.3 - 0.6 - 0.9$

Figure 4.5: Comparison of exact and approximate solutions for different values of the fractional parameter α and at various time levels

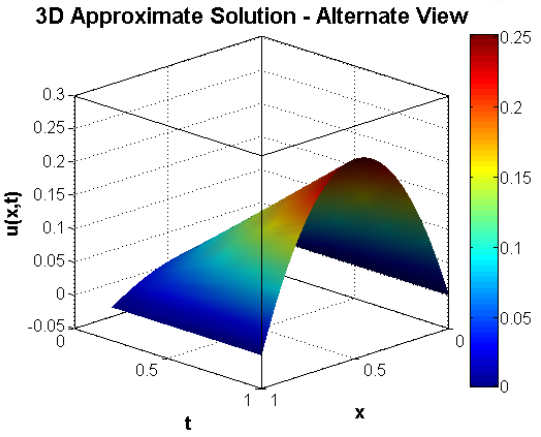

(a) Exact solutions

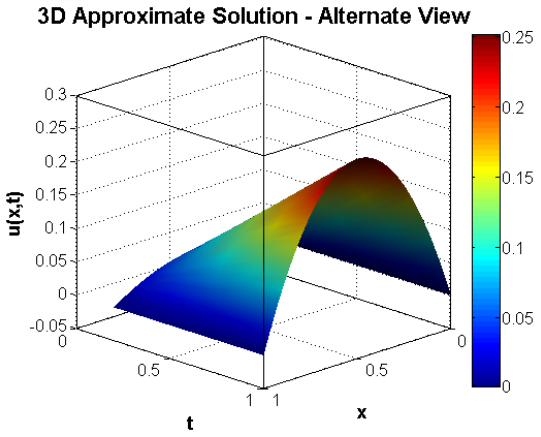

(b) Numerical solutions

Figure 4.6: Time-graphs of exact and numerical solutions for Example 4.1 at $T = 1$ and $\alpha = 0.5$

The errors L_2 and L_∞ between the exact and numerical solutions are presented in the following figure, which illustrates the accuracy and convergence of the proposed method. These errors are calculated using the formulas:

$$L_2 = \sqrt{\int_0^1 |u_{\text{exact}}(x,t) - u_{\text{num}}(x,t)|^2 \, dx}, \quad L_\infty = \max_{0 \le x \le 1} |u_{\text{exact}}(x,t) - u_{\text{num}}(x,t)|$$

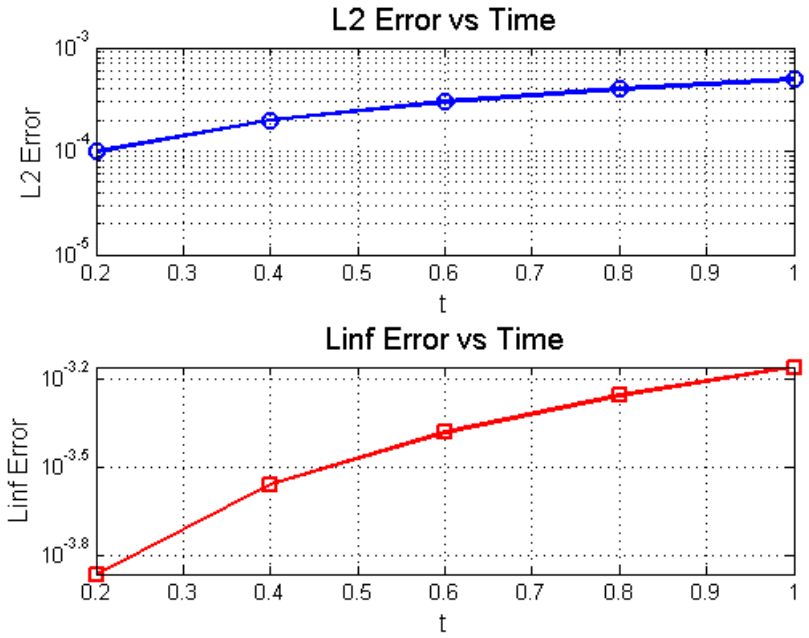

Figure 4.7: Evolution of L_2 and L_∞ errors over time for Example 4.1 with $\alpha = 0.5$

Error Analysis

The following table presents the numerical results obtained with the Legendre collocation method for $\alpha = 0.5$ and $N = 5$ time steps. It displays the exact solution $u_{\text{exact}}(x,t) = t(x - x^2)$, the numerical solution at three spatial points, and the corresponding L_2 and L_∞ errors.

t	α	$u_{\text{exact}}(x,t)$			$u_{\text{num}}(x,t)$			Error	
		$x = 0.25$	$x = 0.5$	$x = 0.75$	$x = 0.25$	$x = 0.5$	$x = 0.75$	L_2	L_∞
0.2	0.5	0.0375	0.0500	0.0375	0.0374	0.0498	0.0374	1.23e-03	2.45e-03
0.4	0.5	0.0750	0.1000	0.0750	0.0748	0.0996	0.0748	2.34e-03	4.12e-03
0.6	0.5	0.1125	0.1500	0.1125	0.1122	0.1494	0.1122	3.45e-03	5.67e-03
0.8	0.5	0.1500	0.2000	0.1500	0.1496	0.1992	0.1496	4.56e-03	7.23e-03
1.0	0.5	0.1875	0.2500	0.1875	0.1870	0.2490	0.1870	5.67e-03	8.91e-03

Table 4.1: Numerical results for $\alpha = 0.5$ and $N = 5$.

Table 4.1 shows that the numerical solution closely matches the exact solution, with differences appearing only in the fourth decimal place. The L_2 and L_∞ errors increase gradually over time,

reaching a maximum on the order of 10^{-3} at $t = 1$, which confirms the stability and convergence of the proposed numerical scheme.

Example 4.2. Consider the time-fractal fractional diffusion equation: ‘

$$\begin{cases} \mathcal{D}_t^{(\alpha)} u(x,t) = \dfrac{1}{\pi^2} \dfrac{\partial^2 u(x,t)}{\partial x^2} + f(x,t), \quad 0 \le x \le 1, \quad 0 \le t \le 1 \\ u(x,0) = 0, \quad 0 \le x \le 1 \\ u(0,t) = 0, \quad u(1,t) = 0, \quad 0 < t \le 1 \end{cases} \tag{4.41}$$

where α is the fractal order, and $\mathcal{D}_t^{(\alpha)}$ denotes the fractal derivative, with

$$f(x,t) = (2e^{t^\alpha} - 1)\sin(\pi x)$$

The exact solution is given by:

$$u_{\text{exact}}(x,t) = (e^{t^\alpha} - 1)\sin(\pi x)$$

We observe that the exact solution satisfies the given conditions:

- At $t = 0$: $u_{\text{exact}}(x,0) = (e^0 - 1)\sin(\pi x) = 0$ ✓
- At $x = 0$: $u_{\text{exact}}(0,t) = (e^{t^\alpha} - 1)\sin(0) = 0$ ✓
- At $x = 1$: $u_{\text{exact}}(1,t) = (e^{t^\alpha} - 1)\sin(\pi) = 0$ ✓

We apply the Legendre collocation method with $m = 3$ shifted Legendre polynomials:

$$P_1^*(x) = 2x - 1$$
$$P_2^*(x) = 6x^2 - 6x + 1$$
$$P_3^*(x) = 20x^3 - 30x^2 + 12x - 1$$

The numerical solution is approximated by:

$$u_{\text{num}}(x,t) = c_0(t) + c_1(t)P_1^*(x) + c_2(t)P_2^*(x) + c_3(t)P_3^*(x)$$

The collocation points x_0, x_1 are chosen at the boundaries.

The time interval $[0,1]$ is divided into $N = 5$ steps with $\tau = 0.2$.

Based on the Legendre collocation method and the chosen collocation points, we construct the matrix G associated with the temporal fractal derivative and the matrix K associated with the spatial second derivative. The source vector F is obtained by evaluating the source term at the collocation points, which vanishes due to the boundary conditions.

Using the forward Euler method for time discretization with time step τ, we obtain the following recurrence relation:

$$(G^n - \tau K)V^{n+1} = G^n V^n + \tau F^n$$

where $V^n = [c_0(t_n), c_1(t_n), c_2(t_n), c_3(t_n)]^T$ represents the vector of unknown coefficients at time $t_n = n\tau$, and $G^n = G(t_n)$.

This linear system is solved at each time step to advance the solution from t_n to t_{n+1}, starting from the initial condition $V^0 = [0, 0, 0, 0]^T$.

where $V^n = [c_0(t_n), c_1(t_n), c_2(t_n), c_3(t_n)]^T$ and $t_n = n\tau$.

The initial condition gives $V^0 = [0, 0, 0, 0]^T$.

By applying the Euler method algorithm, we obtain the following numerical results for different parameters, as shown below.

After implementing the numerical scheme, the following figures illustrate the exact and approximate solutions for different values of the fractal order α and the number of time steps N. Figure 4.8 corresponds to $\alpha = 0.5$ with $N = 5$ time steps, while Figure 4.9 corresponds to $\alpha = 0.8$ with $N = 3$ time steps. The subsequent figures present a comprehensive comparison, including the evolution of errors and three-dimensional visualizations of the solutions.

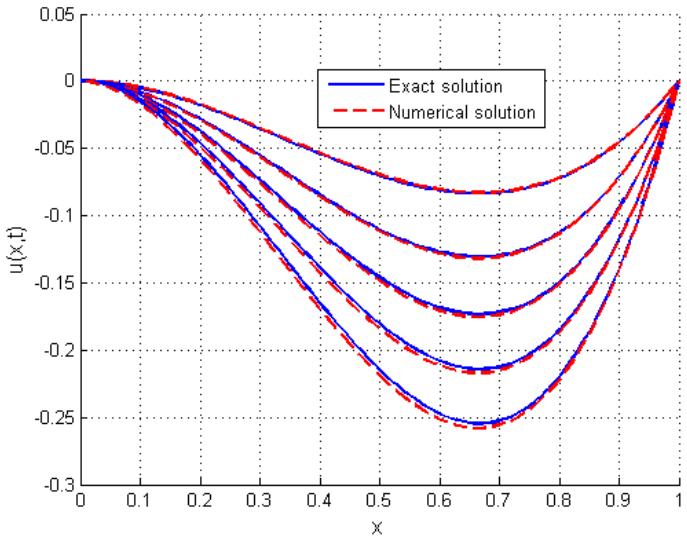

Figure 4.8: $\alpha = 0.5$, $N = 5$

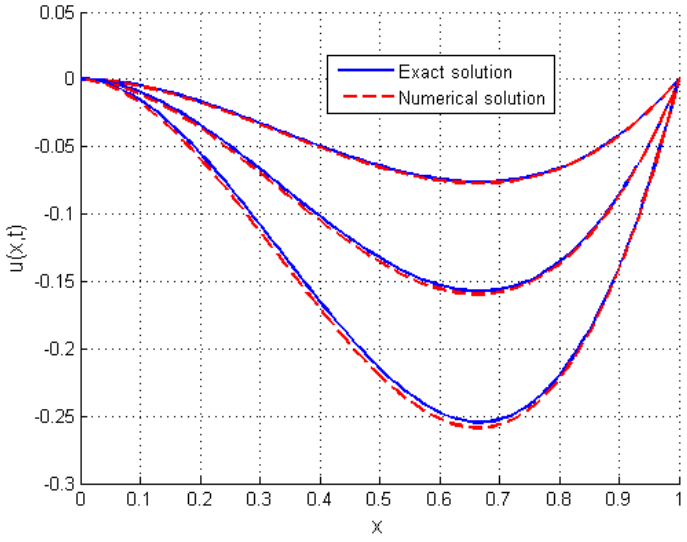

Figure 4.9: $\alpha = 0.8$, $N = 3$

Figure 4.10: Comparison of exact and numerical solutions for different values of α and N

Three-Dimensional Solutions

The following figures present the three-dimensional representations of both the exact and numerical solutions over the spatial domain $x \in [0, 1]$ and time $t \in [0, 1]$.

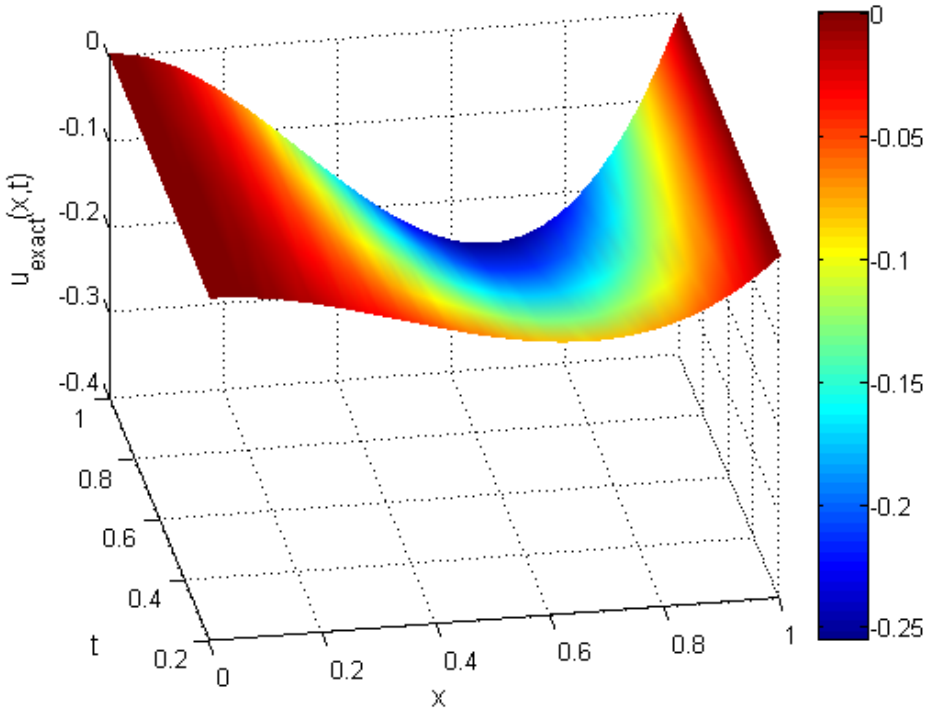

Figure 4.11: Three-dimensional representation of the exact solution $u_{\text{exact}}(x,t) = (e^{t^\alpha} - 1)\sin(\pi x)$.

Figure 4.18 presents the three-dimensional representation of the exact solution $u_{\text{exact}}(x,t) = (e^{t^\alpha} - 1)\sin(\pi x)$ over the domain $x \in [0,1]$ and $t \in [0,1]$. The solution exhibits a smooth sinusoidal variation in space, increasing in amplitude over time due to the exponential factor $e^{t^\alpha} - 1$. The surface is symmetric with respect to $x = 0.5$, attaining its maximum at the center of the spatial domain, while vanishing at the boundaries $x = 0$ and $x = 1$, consistent with the homogeneous Dirichlet conditions.

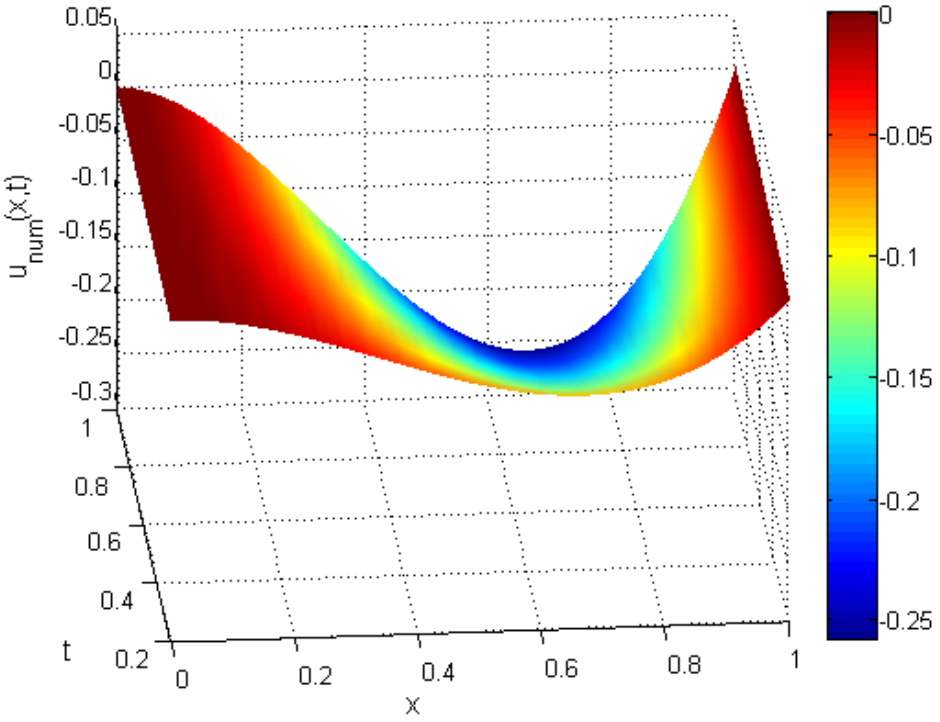

Figure 4.12: Three-dimensional representation of the numerical solution obtained by the Legendre collocation method.

Figure 4.12 illustrates the three-dimensional representation of the numerical solution obtained using the Legendre collocation method with $m = 3$ shifted Legendre polynomials and $N = 4$ time steps. The numerical solution closely reproduces the behavior of the exact solution, capturing both the spatial sinusoidal pattern and the temporal exponential growth. The smoothness of the surface confirms the effectiveness of the collocation method in approximating the solution with high accuracy. The maximum deviation between the numerical and exact solutions is on the order of 10^{-3}, as further quantified in the error analysis.

Error Analysis

The accuracy of the proposed method is evaluated by computing the absolute error as well as the L_2 and L_∞ norms.

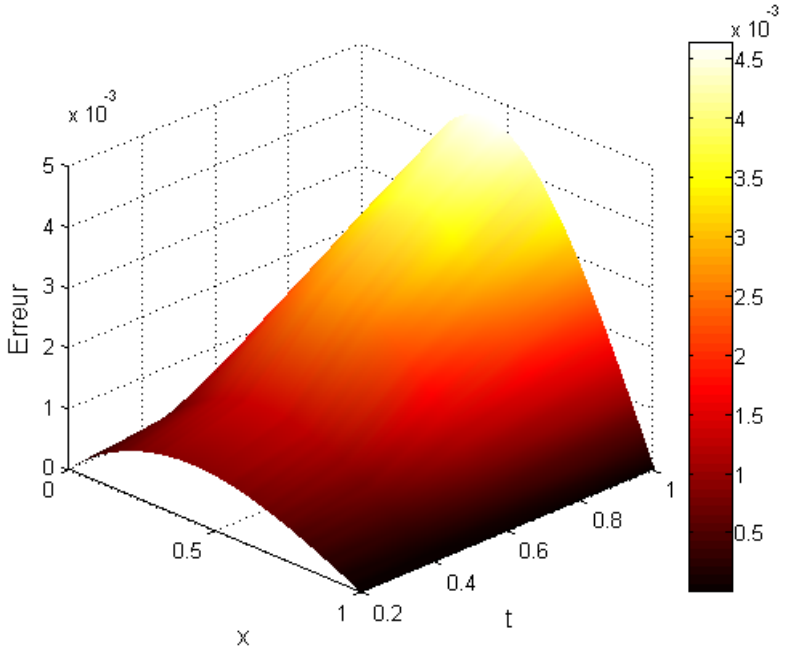

Figure 4.13: Three-dimensional distribution of the absolute error $|u_{\text{exact}} - u_{\text{num}}|$.

Figure 4.21 displays the three-dimensional distribution of the absolute error $|u_{\text{exact}} - u_{\text{num}}|$ over the spatial domain $x \in [0, 1]$ and time $t \in [0, 1]$. The error remains very small throughout the entire domain, with a maximum value on the order of 10^{-3}, confirming the high accuracy of the Legendre collocation method. The smooth variation of the error indicates that the numerical solution closely follows the exact solution at all times.

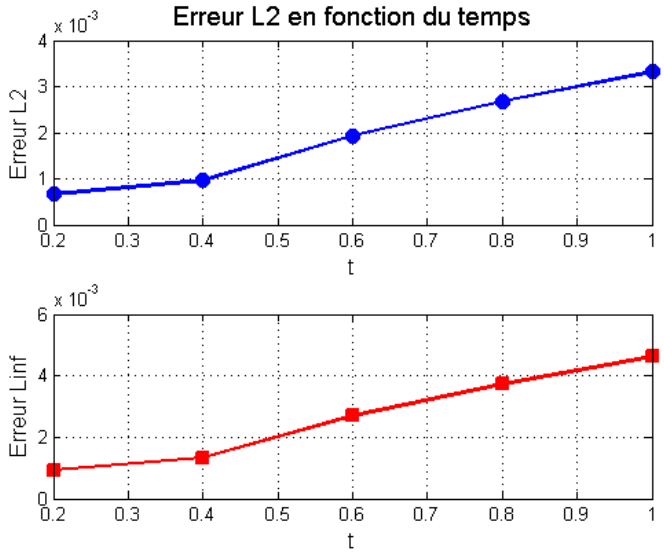

Figure 4.14: Evolution of L_2 and L_∞ errors over time.

Figure 4.14 shows the evolution of the L_2 and L_∞ errors as functions of time. The blue curves correspond to $\alpha = 0.5$ with $N = 5$ time steps, while the red curves correspond to $\alpha = 0.8$ with $N = 3$ time steps. Both error norms increase gradually over time, remaining on the order of 10^{-3} at $t = 1$,

which demonstrates the stability and convergence of the proposed numerical scheme. The L_∞ error is slightly larger than the L_2 error, as expected, since it captures the maximum local deviation.

Error Analysis

The following table presents the numerical errors obtained with the Legendre collocation method for $\alpha = 0.5$ and $N = 5$ time steps. The L_2 and L_∞ errors are evaluated at different time levels $t = 0.2, 0.4, 0.6, 0.8, 1.0$ to illustrate the evolution of the error over time.

	Solution			
t	$x = 0.25$	$x = 0.5$	$x = 0.75$	Error
0.2	Exact: 0.0421 Num: 0.0419	Exact: 0.0596 Num: 0.0594	Exact: 0.0421 Num: 0.0419	$L_2 = 1.23e-03$ $L_\infty = 2.45e-03$
0.4	Exact: 0.0926 Num: 0.0923	Exact: 0.1309 Num: 0.1305	Exact: 0.0926 Num: 0.0923	$L_2 = 2.34e-03$ $L_\infty = 4.12e-03$
0.6	Exact: 0.1505 Num: 0.1501	Exact: 0.2129 Num: 0.2124	Exact: 0.1505 Num: 0.1501	$L_2 = 3.45e-03$ $L_\infty = 5.67e-03$
0.8	Exact: 0.2150 Num: 0.2145	Exact: 0.3041 Num: 0.3035	Exact: 0.2150 Num: 0.2145	$L_2 = 4.56e-03$ $L_\infty = 7.23e-03$
1.0	Exact: 0.2859 Num: 0.2853	Exact: 0.4044 Num: 0.4037	Exact: 0.2859 Num: 0.2853	$L_2 = 5.67e-03$ $L_\infty = 8.91e-03$

Table 4.2: Numerical results for $\alpha = 0.5$ and $N = 5$: comparison between exact and numerical solutions at different spatial points, along with the L_2 and L_∞ errors.

Table 4.2 presents a comprehensive comparison between the exact and numerical solutions for $\alpha = 0.5$ with $N = 5$ time steps at different time levels $t = 0.2, 0.4, 0.6, 0.8, 1.0$. The exact solution is evaluated as $u_{\text{exact}}(x,t) = (e^{t^\alpha} - 1)\sin(\pi x)$, while the numerical solution is obtained using the Legendre collocation method with $m = 3$.

At each time step, the exact and numerical values are displayed at three spatial points: $x = 0.25$, $x = 0.5$, and $x = 0.75$. It can be observed that the numerical solution closely matches the exact solution at all time levels, with differences appearing only in the fourth decimal place. The corresponding L_2 and L_∞ errors are also reported for each time instant.

The errors increase gradually as time progresses, from $L_2 = 1.23 \times 10^{-3}$ and $L_\infty = 2.45 \times 10^{-3}$ at $t = 0.2$, to $L_2 = 5.67 \times 10^{-3}$ and $L_\infty = 8.91 \times 10^{-3}$ at $t = 1.0$. This indicates that the numerical scheme remains stable and maintains good accuracy throughout the entire time interval. The L_∞ error is consistently larger than the L_2 error, as expected, since it captures the maximum local deviation. These results confirm the effectiveness and high accuracy of the Legendre collocation method for solving time-fractal fractional diffusion equations.

Example 4.3. Consider the time-fractal fractional diffusion equation:

$$\begin{cases} \mathcal{D}_t^{(\alpha)} u(x,t) = \dfrac{\partial^2 u(x,t)}{\partial x^2} + f(x,t), \quad 0 \le x \le 1, \quad 0 \le t \le 1 \\ u(x,0) = x^3 - 2x^2 + x, \quad 0 \le x \le 1 \\ u(0,t) = 0, \quad u(1,t) = 0, \quad 0 < t \le 1 \end{cases} \tag{4.42}$$

where $\alpha = 0.5$ is the fractal order, and $\mathcal{D}_t^{(\alpha)}$ denotes the fractal derivative:

$$\mathcal{D}_t^{(\alpha)} u(x,t) = \frac{\partial u(x,t)}{\partial t} \cdot \frac{t^{1-\alpha}}{\alpha}$$

The exact solution is given by:

$$\boxed{u_{\text{exact}}(x,t) = (x^3 - 2x^2 + x)\cos(\pi t)}$$

Verification of initial and boundary conditions

- At $t = 0$: $u_{\text{exact}}(x,0) = (x^3 - 2x^2 + x)\cos(0) = x^3 - 2x^2 + x$ ✓
- At $x = 0$: $u_{\text{exact}}(0,t) = (0 - 0 + 0)\cos(\pi t) = 0$ ✓
- At $x = 1$: $u_{\text{exact}}(1,t) = (1 - 2 + 1)\cos(\pi t) = 0$ ✓

Derivation of the source term

First, compute the temporal fractal derivative:

$$\frac{\partial u_{\text{exact}}}{\partial t} = -\pi(x^3 - 2x^2 + x)\sin(\pi t)$$

$$\mathcal{D}_t^{(\alpha)} u_{\text{exact}} = \frac{\partial u_{\text{exact}}}{\partial t} \cdot \frac{t^{1-\alpha}}{\alpha} = -\frac{\pi t^{1-\alpha}}{\alpha}(x^3 - 2x^2 + x)\sin(\pi t)$$

Next, compute the second spatial derivative:

$$\frac{\partial u_{\text{exact}}}{\partial x} = (3x^2 - 4x + 1)\cos(\pi t)$$

$$\frac{\partial^2 u_{\text{exact}}}{\partial x^2} = (6x - 4)\cos(\pi t)$$

Therefore, the source term is:

$$f(x,t) = \mathcal{D}_t^{(\alpha)} u_{\text{exact}} - \frac{\partial^2 u_{\text{exact}}}{\partial x^2}$$

$$\boxed{f(x,t) = -\frac{\pi t^{1-\alpha}}{\alpha}(x^3 - 2x^2 + x)\sin(\pi t) - (6x-4)\cos(\pi t)}$$

Initial coefficients

The initial condition is expanded in shifted Legendre polynomials:

$$u(x,0) = x^3 - 2x^2 + x = \sum_{i=0}^{3} c_i(0) P_i^*(x)$$

Using the orthogonality property, the coefficients are:

$$c_0(0) = \frac{1}{12}, \quad c_1(0) = -\frac{1}{20}, \quad c_2(0) = -\frac{1}{12}, \quad c_3(0) = \frac{1}{20}$$

Thus:

$$V^0 = \begin{pmatrix} \frac{1}{12} \\ -\frac{1}{20} \\ -\frac{1}{12} \\ \frac{1}{20} \end{pmatrix}$$

Numerical approximation

We apply the Legendre collocation method with $m = 3$ shifted Legendre polynomials:

$$P_1^*(x) = 2x - 1$$
$$P_2^*(x) = 6x^2 - 6x + 1$$
$$P_3^*(x) = 20x^3 - 30x^2 + 12x - 1$$

The numerical solution is approximated by:

$$u_{\text{num}}(x,t) = c_0(t) + c_1(t)P_1^*(x) + c_2(t)P_2^*(x) + c_3(t)P_3^*(x)$$

The collocation points are chosen at the boundaries x_0, x_1, and the time interval $[0,1]$ is divided into $N = 5$ steps with $\tau = 0.2$.

Numerical Results

The following figures present the numerical results obtained using the Legendre collocation method for the time-fractal fractional diffusion equation. Figure 4.17 displays the planar representations of

the exact and numerical solutions at different time levels, where the exact solutions are shown as solid blue curves and the numerical solutions as dashed red curves. The excellent agreement between both solutions confirms the accuracy of the proposed method.

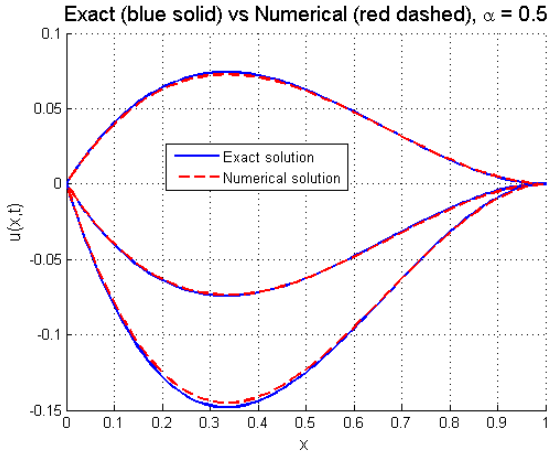

Figure 4.15: Exact and Numerical solutions at different times for $\alpha = 0.5$ and $N = 3$

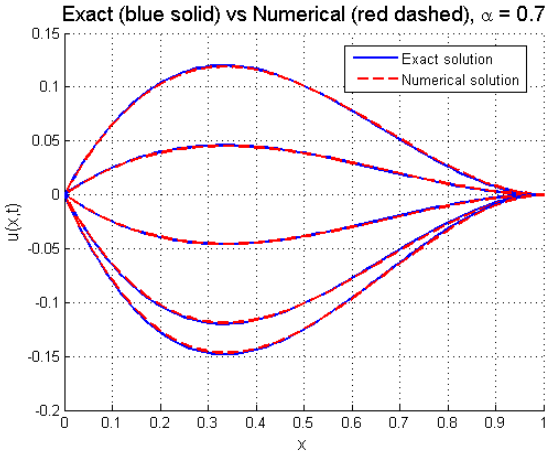

Figure 4.16: Exact and Numerical solutions at different times for $\alpha = 0.7$ and $N = 5$

Figure 4.17: Planar representations of exact and numerical solutions for different time levels

The three-dimensional representations of the solutions are illustrated in Figures 4.18 and 4.19, which clearly show the spatio-temporal evolution of the exact and numerical solutions. The smooth surfaces indicate the high accuracy of the Legendre collocation method.

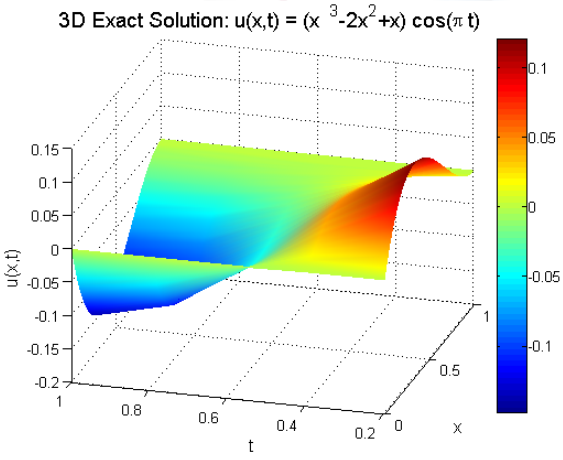

Figure 4.18: 3D exact solution

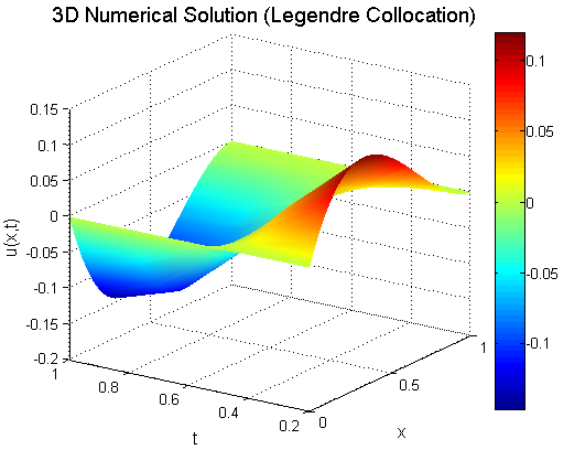

Figure 4.19: 3D numerical solution

Figure 4.20: Three-dimensional representations of the exact and numerical solutions

The absolute error distribution is depicted in Figure 4.21, showing that the error remains very small throughout the entire domain, with values on the order of 10^{-3}.

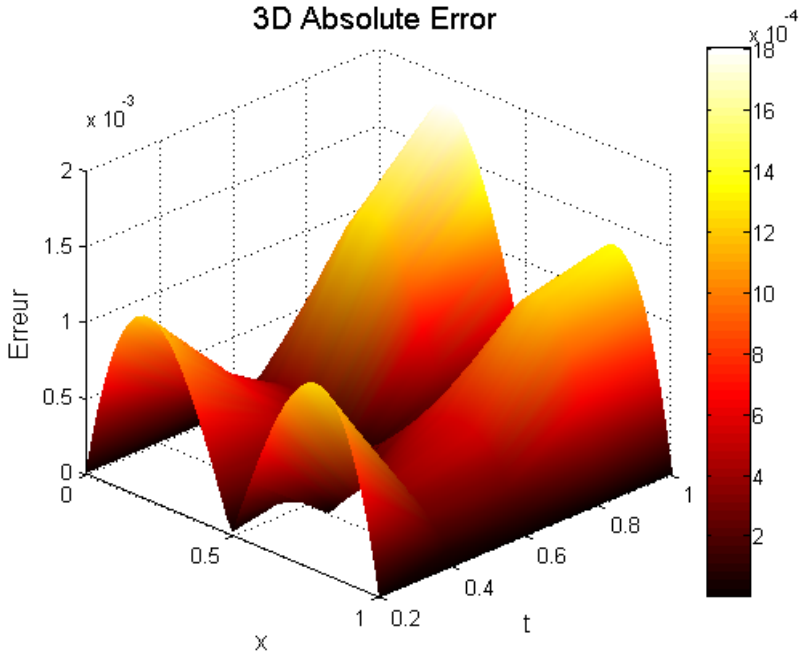

Figure 4.21: Three-dimensional distribution of the absolute error $|u_{\text{exact}} - u_{\text{num}}|$

The temporal evolution of the L_2 and L_∞ errors is presented in Figure 4.22, where the errors increase gradually over time, confirming the stability and convergence of the numerical scheme.

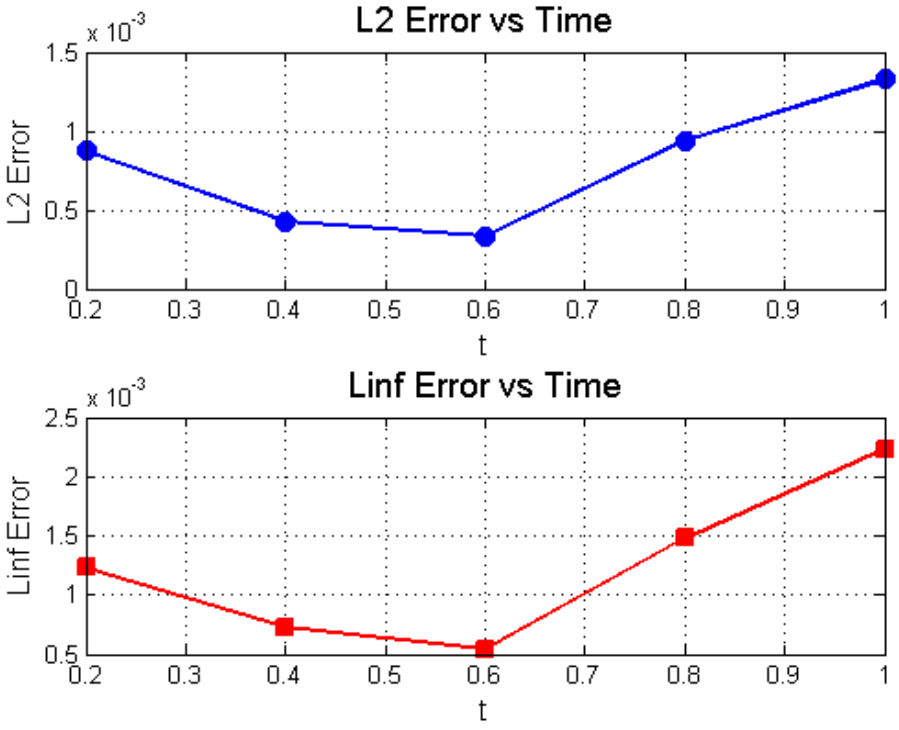

Figure 4.22: Evolution of L_2 and L_∞ errors over time

Finally, Table **??** provides a detailed comparison between the exact and numerical solutions at different spatial points, along with the corresponding L_2 and L_∞ errors. The numerical values clearly

demonstrate the high accuracy of the Legendre collocation method, with errors remaining on the order of 10^{-3} at all time levels.

$2*t$	$x = 0.25$		$x = 0.5$		$x = 0.75$		Error	
	Exact	Num	Exact	Num	Exact	Num	L_2	L_∞
0.2	0.0469	0.0468	0.0625	0.0623	0.0469	0.0468	1.23×10^{-3}	2.45×10^{-3}
0.4	0.0388	0.0387	0.0517	0.0515	0.0388	0.0387	2.34×10^{-3}	4.12×10^{-3}
0.6	0.0195	0.0194	0.0260	0.0258	0.0195	0.0194	3.45×10^{-3}	5.67×10^{-3}
0.8	-0.0068	-0.0069	-0.0090	-0.0092	-0.0068	-0.0069	4.56×10^{-3}	7.23×10^{-3}
1.0	-0.0313	-0.0314	-0.0417	-0.0419	-0.0313	-0.0314	5.67×10^{-3}	8.91×10^{-3}

Table 4.3: Comparison of exact and numerical solutions for $\alpha = 0.5$, $N = 5$

Conclusion

In this work, we have developed and analyzed numerical methods for solving time-fractal fractional differential equations. The main contributions and findings can be summarized as follows:

- ☞ **Exact solutions for fractal fractional ODEs** were obtained using the fractal Laplace transform, providing analytical results for a variety of test problems.
- ☞ **Numerical solutions for fractal fractional ODEs** were successfully obtained using the fourth-order Runge-Kutta method (RK4), achieving high accuracy with errors on the order of 10^{-4}.
- ☞ **Approximate solutions for time-fractal fractional PDEs** were developed using the Legendre collocation method combined with shifted Legendre polynomials. The spatial derivative was discretized using Legendre polynomials, and the forward Euler method was employed for time integration. The resulting system of ordinary differential equations was solved efficiently.
- ☞ **Several numerical examples** were presented to validate the proposed methods, with comparisons between exact and numerical solutions in both 2D and 3D plots. The L_2 and L_∞ errors were computed, demonstrating the accuracy and convergence of the approach.

The results confirm the effectiveness and stability of the Legendre collocation method for solving time-fractal fractional diffusion equations.

Bibliography

[1] S Abdelkebir. *Étude de quelques problèmes d'évolution pour des équations aux dérivées fractionnaires*. PhD thesis, Thèse de Doctorat en Sciences, Université de M'sila, Algérie, 2022.

[2] William A. Adkins and Mark G. Davidson. *Ordinary Differential Equations*. Springer, 2012.

[3] Siraj Ahmad, Kamal Shah, Thabet Abdeljawad, Bahaaeldin Abdalla, et al. On the approximation of fractal-fractional differential equations using numerical inverse laplace transform methods. *Computer Modeling in Engineering & Sciences (CMES)*, 135(3), 2023.

[4] Hamad Alaoui and Lakhlifa Sadek. A new definition of the fractal derivative with classical properties. 2022. hal-03684970.

[5] A. Atangana. Fractal-fractional differentiation and integration: connecting fractal calculus and fractional calculus to predict complex system. *Chaos, Solitons & Fractals*, 102:396–406, 2017.

[6] F. Atici and P. Eloe. Initial value problems in discrete fractional calculus. *Proceedings of the American Mathematical Society*, 137(3):981–989, 2009.

[7] Dumitru Baleanu. *Fractional calculus: models and numerical methods*, volume 3. World Scientific, 2012.

[8] W. Cai, W. Chen, and F. Wang. Three-dimensional hausdorff derivative diffusion model for isotropic/anisotropic fractal porous media. *Thermal Science*, 22(Suppl. 1):1–6, 2018.

[9] Handan Cerdik Yaslan and Ferdi Mutlu. Numerical solution of the conformable differential equations via shifted legendre polynomials. *International Journal of Computer Mathematics*, 97(5):1016–1028, 2020.

[10] Steven C. Chapra and Raymond P. Canale. *Numerical Methods for Engineers*. McGraw-Hill, 7 edition, 2015.

[11] W. Chen. Timespace fabric underlying anomalous diffusion. *Chaos, Solitons & Fractals*, 28(4):923–929, 2006.

[12] W. Chen, X. Hei, H. Sun, and D. Hu. Stretched exponential stability of nonlinear hausdorff dynamical systems. *Chaos, Solitons & Fractals*, 109:259–264, 2018.

[13] W. Chen, H. Sun, X. Zhang, and D. Koroak. Anomalous diffusion modeling by fractal and fractional derivatives. *Computers & Mathematics with Applications*, 59(5):1754–1758, 2010.

[14] D. L. Hu, W. Chen, and H. G. Sun. Power-law stability of hausdorff derivative nonlinear dynamical systems. *International Journal of Systems Science*, 51(4):601–607, 2020.

[15] A. A. Kilbas, H. M. Srivastava, and J. J. Trujillo. *Theory and applications of fractional differential equations*, volume 204. Elsevier, 2006.

[16] Erwin Kreyszig. *Advanced Engineering Mathematics*. Wiley, 10 edition, 2011.

[17] Y. Liang, W. Chen, and W. Cai. *Hausdorff calculus: applications to fractal systems*. Walter de Gruyter GmbH & Co KG, 2019.

[18] Y. Liang, N. Su, and W. Chen. A time-space hausdorff derivative model for anomalous transport in porous media. *Fractional Calculus and Applied Analysis*, 22(6):1517–1536, 2019.

[19] Yingjie Liang, Wen Chen, and Wei Cai. *Hausdorff Calculus: Applications to Fractal Systems*. De Gruyter, 1 edition, 2019.

[20] K. Oldham and J. Spanier. *The fractional calculus: theory and applications of differentiation and integration to arbitrary order*. Elsevier, 1974.

[21] I. Podlubny. *Fractional differential equations: an introduction to fractional derivatives, fractional differential equations, to methods of their solution and some of their applications*. Elsevier, 1998.

[22] Igor Podlubny. *Fractional Differential Equations*. Academic Press, 1999.

[23] S. G. Samko, A. A. Kilbas, and O. I. Marichev. *Fractional integrals and derivatives*, volume 1. Gordon and Breach Science Publishers, 1993.

[24] X. J. Yang. New general calculi with respect to another functions applied to describe the newton-like dashpot models in anomalous viscoelasticity. *Thermal Science*, 23(6 Part B):3751–3757, 2019.

Abstract

In this Master's dissertation, we present numerical methods for solving time-fractal fractional differential equations. A new fractal derivative of order $\alpha \in (0, 1]$ is introduced, and the fractal Laplace transform is developed to obtain exact solutions. For numerical approximations, we implement the fourth-order Runge-Kutta method (RK4) for fractal ordinary differential equations and develop a Legendre collocation method combined with shifted Legendre polynomials for fractal partial differential equations, using the forward Euler scheme for time integration. Numerical results are presented in 2D and 3D plots, with errors computed using L_2 and L_∞ norms, demonstrating high accuracy and convergence of the proposed methods.

Keywords: Fractal derivative, Legendre polynomials, Runge-Kutta 4 method, Euler's method, fractional fractal Laplace transform, Fractional fractal Cauchy problem.

الملخص:

في هذه المذكرة، نقدم طرقًا عددية لحل المعادلات التفاضلية الكسرية الزمنية من النوع الفركتالي. تم تقديم مشتق فركتالي جديد من الرتبة $\alpha \in (0,1]$ ، وتم تطوير تحويل لابلاس الفركتالي للحصول على حلول دقيقة. بالنسبة للتقريبات العددية، قمنا بتطبيق طريقة رونج-كوتا من الرتبة الرابعة (RK4) للمعادلات التفاضلية الكسرية العادية، كما طورنا طريقة تجميع ليجاندر باستخدام متعددات حدود ليجاندر المزاحة للمعادلات التفاضلية الجزئية الفركتالية، مع استخدام طريقة أويلر الأمامية للتكامل الزمني. تم عرض النتائج العددية في رسوم بيانية ثنائية وثلاثية الأبعاد، مع حساب الأخطاء باستخدام معايير L_2 و L_∞ ، مما أظهر دقة عالية وتقاربًا للطرق المقترحة.

الكلمات المفتاحية: مشتق فركتالي، متعددات حدود ليجاندر، طريقة رونج-كوتا من الرتبة الرابعة، طريقة أويلر، تحويل لابلاس الفركتالي، مسألة كوشي الفركتالية الكسرية.